

A FAST, STRONG, TOPOLOGICALLY MEANINGFUL, AND FUN KNOT INVARIANT

DROR BAR-NATAN AND ROLAND VAN DER VEEN

ABSTRACT. In this paper we discuss a pair of polynomial knot invariants $\Theta = (\Delta, \theta)$ which is:

- Theoretically and practically fast: Θ can be computed in polynomial time. We can compute it in full on random knots with over 300 crossings, and its evaluation at simple rational numbers on random knots with over 600 crossings.
- Strong: Its separation power is much greater than the hyperbolic volume, the HOMFLY-PT polynomial and Khovanov homology (taken together) on knots with up to 15 crossings (while being computable on much larger knots).
- Topologically meaningful: It gives a genus bound, and there are reasons to hope that it would do more.
- Fun: Scroll to Figures 1.1–1.4 and 3.1.

Δ is merely the Alexander polynomial. θ is almost certainly equal to an invariant that was studied extensively by Ohtsuki [Oh2], continuing Rozansky, Kricker, and Garoufalidis [Roz1, Roz2, Roz3, Kr, GR]. Yet our formulas, proofs, and programs are much simpler and enable its computation even on very large knots.

CONTENTS

1. Fun	2
2. The Main Theorem	4
3. Implementation and Examples	8
3.1. Implementation	8
3.2. Examples	9
4. Proof of Invariance	12
5. Strong and Meaningful	21
5.1. Strong	21
5.2. Meaningful	23
5.2.1. The Knot Genus	23
5.2.2. Fibered Knots	24
6. Stories, Conjectures, and Dreams	24
References	30

Date: First edition Not Yet. This edition August 27, 2025.


2020 Mathematics Subject Classification. Primary 57K14, secondary 16T99.

Key words and phrases. Alexander polynomial, ~~NOTE~~.

This work was partially supported by NSERC grant RGPIN-2018-04350 and by the Chu Family Foundation (NYC). It is available in electronic form, along with source files and a demo *Mathematica* notebook at <http://drorbn.net/Theta> and at [arXiv:2508.18111](https://arxiv.org/abs/2508.18111).

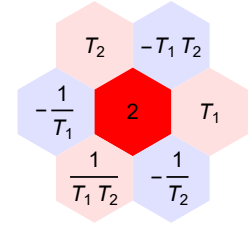
1. FUN

The word “fun” rarely appears in the title of a math paper, so let us start with a brief justification.

Θ is a pair of polynomials. The first, Δ , is old news, the Alexander polynomial [Al]. It is a one-variable Laurent polynomial in a variable T . For example, $\Delta(\textcircled{3}) = T^{-1} - 1 + T$. We turn such a polynomial into a list of coefficients (for $\textcircled{3}$, it is $(1, -1, 1)$), and then to a chain of bars of varying colours: white for the zero coefficients, and red and blue for the positive and negative coefficients (with intensity proportional to the magnitude of the coefficients). The result is a “bar code”, and for the trefoil $\textcircled{3}$ it is .

Similarly, θ is a 2-variable Laurent polynomial, in variables T_1 and T_2 . We can turn such a polynomial into a 2D array of coefficients and then using the same rules, into a 2D array of colours, namely, into a picture. To highlight a certain conjectured hexagonal symmetry of the resulting pictures, we apply a shear transformation to the plane before printing.

So a monomial $cT_1^{n_1}T_2^{n_2}$ gets printed at position $(n_1 - n_2/2, \sqrt{3}n_2/2)$ instead of the more traditional (n_1, n_2) . On the right is the 2D picture corresponding to the polynomial $2 + T_1 - T_1T_2 + T_2 - T_1^{-1} + T_1^{-1}T_2^{-1} - T_2^{-1}$.



Thus Θ becomes a pair of pictures: a bar code, and a 2D picture that we call a “hexagonal QR code”. For the knots in the Rolfsen table (with the unknot prepended at the start), they are in Figure 1.1. For some alternating square weave knots, they are in Figure 1.2, and for a random square weave, in Figure 1.3. In addition, the hexagonal QR codes of 15 knots with ≥ 300 crossings are in Figure 1.4, and Θ of a 132-crossing torus knot is in Figure 3.1.

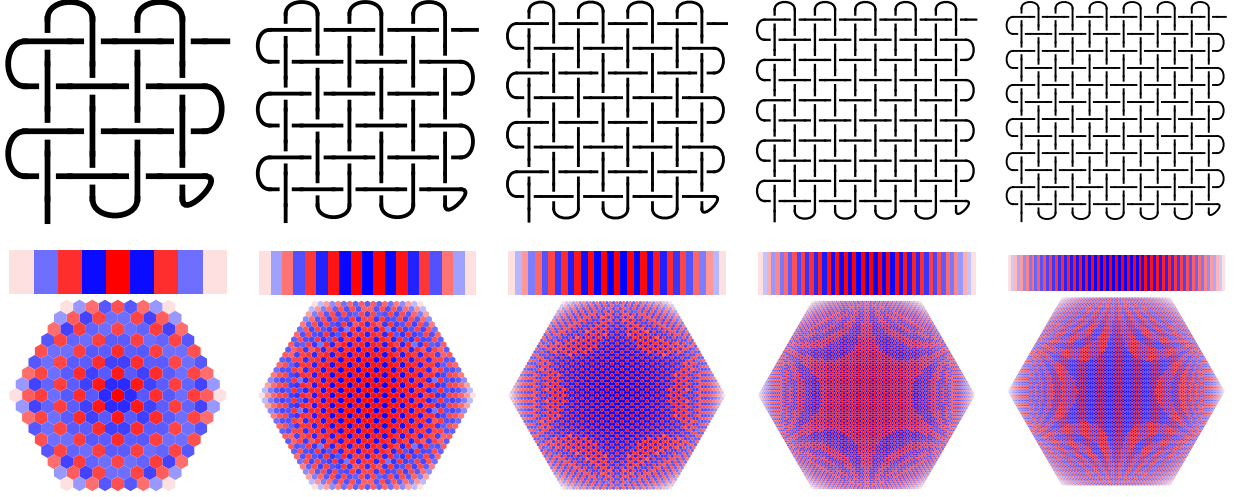
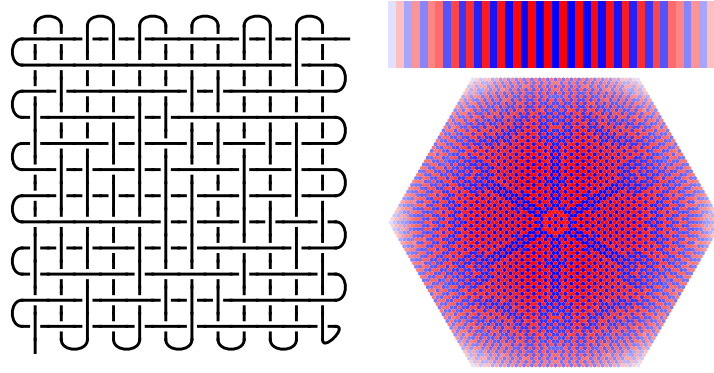
Clearly there are patterns in these figures. There is a hexagonal symmetry and the QR codes are nearly always hexagons (these are independent properties). Much more can be seen in Figure 1.1. In Figure 1.4 there seem to be large-scale patterns perhaps reminiscent of the “Chladni figures” formed by powders atop vibrating plates (on right). We can’t prove any of these things, and the last one, we can’t even formulate properly. Yet they are clearly there, too clear to be the result of chance alone.

We plan to have fun over the next few years observing and proving these patterns. We hope that others will join us too.



left: © Whipple Museum of the History of Science, University of Cambridge; right: CC-BY-SA 4.0 / Wikimedia / Matematica (IME USP) / Rodrigo Tetsuo Argenton

FIGURE 1.1. Θ as a bar code and a QR code, for all the knots in the Rolfsen table.

FIGURE 1.2. Θ of some square weave knots, as computed by [BV3, WeaveKnots.nb].FIGURE 1.3. Θ of a randomized weave knot, as computed by [BV3, WeaveKnots.nb]. Crossings were chosen to be positive or negative with equal probabilities.

2. THE MAIN THEOREM

Given an oriented n -crossing knot K , we draw it in the plane as a long knot diagram D in such a way that the two strands intersecting at each crossing are pointing up (that's always possible because we can always rotate crossings as needed), and so that at its beginning and at its end the knot is oriented upward. We call such a diagram an *upright knot diagram*. An example of an upright knot diagram is shown on the right.

We then label each edge of the diagram with two labels: a running index k which runs from 1 to $2n + 1$, and a “rotation number” φ_k , the geometric rotation number of that edge¹. On

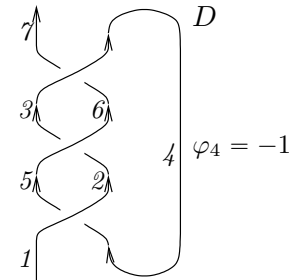


FIGURE 2.1. An example upright knot diagram.

¹The signed number of times the tangent to the edge is horizontal and heading right, with cups counted with +1 signs and caps with -1; this number is well defined because at their ends, all edges are headed up.

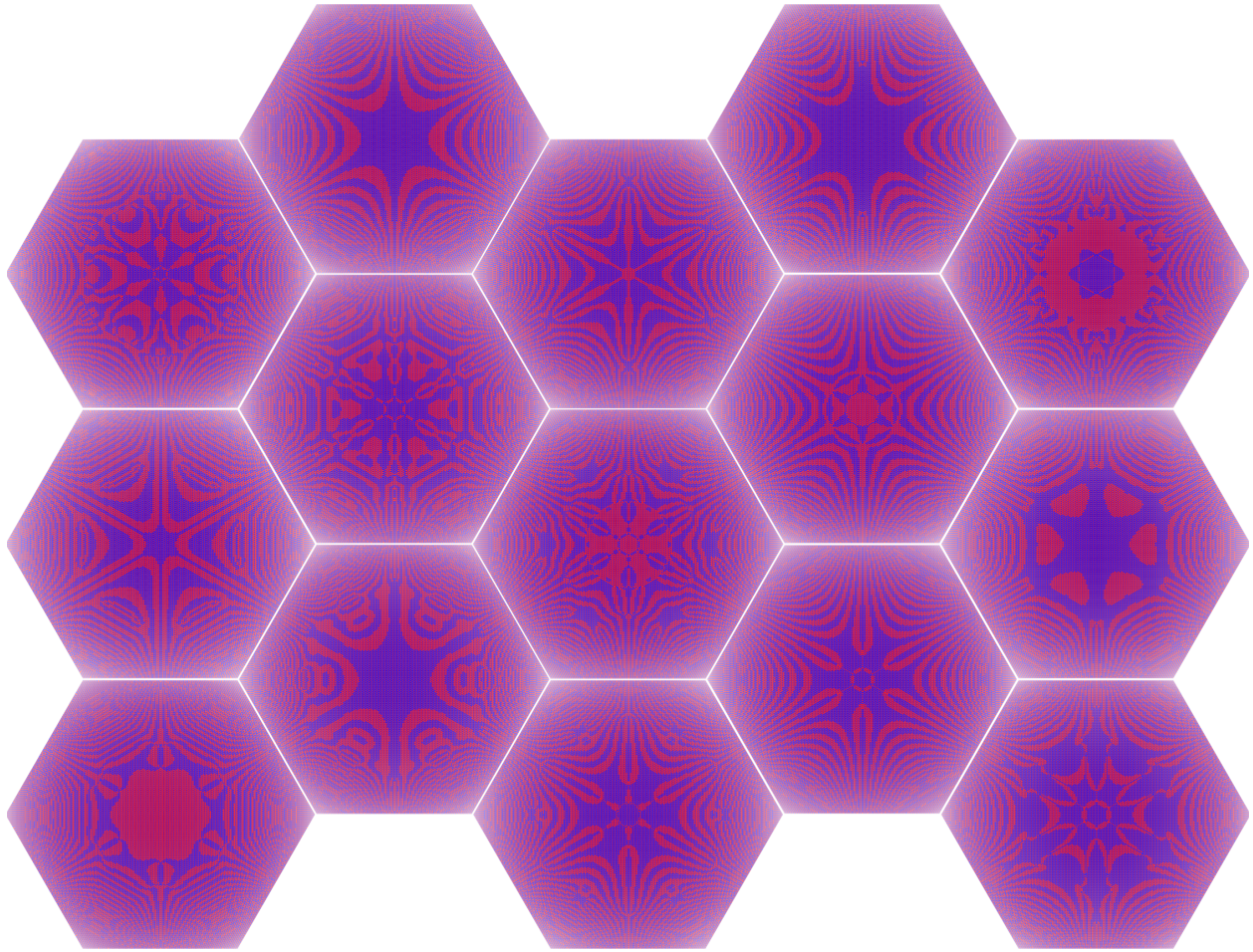


FIGURE 1.4. θ (hexagonal QR code only) of the 15 largest knots that we have computed by September 16, 2024. They are all “generic” in as much as we know, and they all have ≥ 300 crossings. The knots come from [DHOEBL]. Warning: Some screens/printers may introduce spurious Moiré interference patterns.

Figure 2.1

the right the running index runs from 1 to 7, and the rotation numbers for all edges are 0 (and hence are omitted) except for φ_4 , which is -1 .

Let X be the set of all crossings in the diagram D , where we encode each crossing as a triple (sign, incoming over edge, incoming under edge). In our example we have $X = \{(1, 1, 4), (1, 5, 2), (1, 3, 6)\}$.

We let A be the $(2n+1) \times (2n+1)$ matrix of Laurent polynomials in a variable T , defined by

$$A := I - \sum_{c=(s,i,j) \in X} (T^s E_{i,i+1} + (1 - T^s) E_{i,j+1} + E_{j,j+1}),$$

where I is the identity matrix and $E_{\alpha\beta}$ denotes the elementary matrix with 1 in row α and column β and zeros elsewhere.

Alternatively, $A = I + \sum_c A_c$, where A_c is a matrix of zeros except for the blocks as follows:

$$\begin{array}{ccc} \begin{array}{c} j+1 \nearrow \quad \nearrow i+1 \\ i \searrow \quad \searrow j \\ s = +1 \end{array} & \begin{array}{c} i+1 \nearrow \quad \nearrow j+1 \\ j \searrow \quad \searrow i \\ s = -1 \end{array} & \longrightarrow \begin{array}{c|cc} A_c & \text{column } i+1 & \text{column } j+1 \\ \hline \text{row } i & -T^s & T^s - 1 \\ \text{row } j & 0 & -1 \end{array} \end{array} \quad (1)$$

We note that the determinant of A is equal up to a unit to the normalized Alexander polynomial Δ of K .² In fact, we have that

$$\Delta = T^{(-\varphi(D) - w(D))/2} \det(A), \quad (2)$$

where $\varphi(D) := \sum_k \varphi_k$ is the total rotation number of D and where $w(D) = \sum_c s_c$ is the writhe of D , namely the sum of the signs s_c of all the crossings c in D .

We let $G = (g_{\alpha\beta}) = A^{-1}$ and, thinking of it as a function $g_{\alpha\beta}$ of a pair of edges α and β , we call it the Green function of the diagram D . When inspired by physics (e.g. [BN5]) we sometimes call it “the 2-point function”, and when thinking of car traffic (e.g. [BV1, BN6]) we sometimes call it “the traffic function”.

Let T_1 and T_2 be indeterminates and let $T_3 := T_1 T_2$. Let $\Delta_\nu := \Delta|_{T \rightarrow T_\nu}$ and $G_\nu = (g_{\nu\alpha\beta}) := G|_{T \rightarrow T_\nu}$ be Δ and G subject to the substitution $T \rightarrow T_\nu$, where $\nu = 1, 2, 3$.

Given crossings $c = (s, i, j)$, $c_0 = (s_0, i_0, j_0)$, and $c_1 = (s_1, i_1, j_1)$ in X and an edge label k , let

$$\begin{aligned} F_1(c) = & s [1/2 - g_{3ii} + T_2^s g_{1ii} g_{2ji} - T_2^s g_{3jj} g_{2ji} - (T_2^s - 1) g_{3ii} g_{2ji} \\ & + (T_3^s - 1) g_{2ji} g_{3ji} - g_{1ii} g_{2jj} + 2 g_{3ii} g_{2jj} + g_{1ii} g_{3jj} - g_{2ii} g_{3jj}] \\ & + \frac{s}{T_2^s - 1} [(T_1^s - 1) T_2^s (g_{3jj} g_{1ji} - g_{2jj} g_{1ji} + T_2^s g_{1ji} g_{2ji}) \\ & + (T_3^s - 1) g_{3ji} (1 - T_2^s g_{1ii} + g_{2ij} + (T_2^s - 2) g_{2jj} - (T_1^s - 1)(T_2^s + 1) g_{1ji})], \end{aligned} \quad (3)$$

$$F_2(c_0, c_1) = \frac{s_1 (T_1^{s_0} - 1) (T_3^{s_1} - 1) g_{1j_1 i_0} g_{3j_0 i_1}}{T_2^{s_1} - 1} (T_2^{s_0} g_{2i_1 i_0} + g_{2j_1 j_0} - T_2^{s_0} g_{2j_1 i_0} - g_{2i_1 j_0}) \quad (4)$$

$$F_3(k) = (g_{3kk} - 1/2) \varphi_k \quad (5)$$

These formulas are uninspiring, yet they are easy to compute (given G), and they work:

Theorem 1 (The Main Theorem, proof in Section 4). *The following is a knot invariant:*

$$\theta(D) := \Delta_1 \Delta_2 \Delta_3 \left(\sum_{c \in X} F_1(c) + \sum_{c_0, c_1 \in X} F_2(c_0, c_1) + \sum_{\text{edges } k} F_3(k) \right). \quad (6)$$

Some comments are now in order:

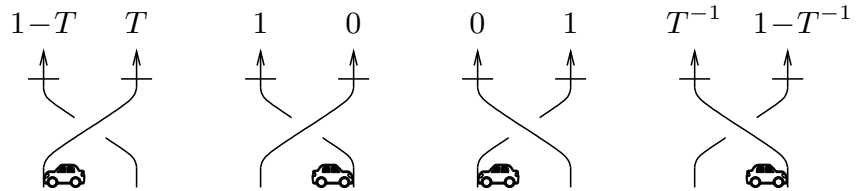
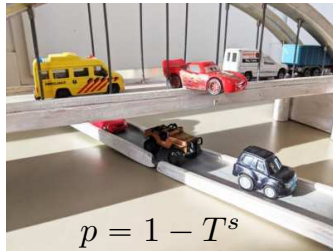
Comment 2. We note following [BV1] that $g_{\alpha\beta}$ can be interpreted as measuring “car traffic”, assuming a stream of traffic is injected near the start of edge α and a “traffic counter” is placed near the end of edge β , and where cars always obey the following traffic rules:

- Car travel on the edges of the knot, always in a direction consistent with the orientation of these edges.

²The informed reader will note that A is a presentation matrix for the Alexander module of K , obtained by using Fox calculus on the Wirtinger presentation of the fundamental group of the complement of K .

- When a car reaches a crossing on the under-strand, it travels through and continues on the other side.
- When a car reaches a crossing of sign $s = \pm 1$ on the over-strand, it continues right through with probability T^s , yet with probability $1 - T^s$ it falls down and continues travelling on the lower strand. (It matters not that T and T^{-1} cannot be probabilities at the same time — we merely use the algebraic rules of probability without caring about the inequalities that normally come with them).
- When cars reach the “end” of the knot, the abyss that follows edge $2n + 1$, they fall the picture never to be seen again.

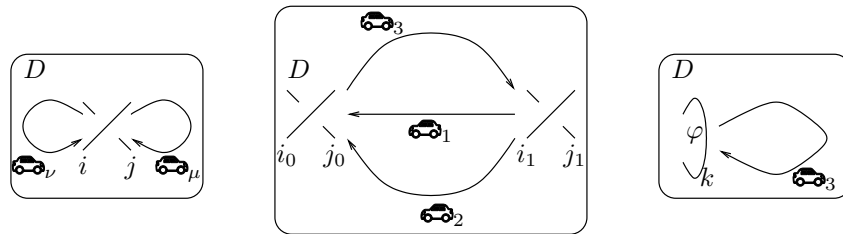
These rules can be summarized by the following pictures:



For further details, see [BV1].

2

Comment 3. We note without detail that there is an alternative formula for θ in terms of perturbed Gaussian integration [BN5]. In that language, and using also the traffic motifs of Discussion 2, the three summands in (6) become Feynman diagrams for processes in which cars car_ν governed by parameter $T_\nu = T_1, T_2$, or T_3 interact:



In particular, the middle diagram which resembles the Greek letter Θ gave the invariant its name.

3

Comment 4. The computation of G is a bottleneck for the computation of Θ . It requires inverting a $(2n + 1) \times (2n + 1)$ matrix whose entries are (degree 1) Laurent polynomials in T . It's a daunting task yet it takes polynomial time, it can be performed in practice even if n is in the hundreds, and everything which then follows is easier.




Computationally, the worst term in (6) is the middle one, and even it takes merely $\sim n^2$ operations in the ring $\mathbb{Q}(T_1, T_2)$ to complete.



The polynomials $F_1(c)$, $F_2(c_0, c_1)$ and $F_3(k)$ are not unique, and we are not certain that we have the cleanest possible formulas for them. They are ugly from a human perspective, yet from a computational perspective, having 18 terms (as is the case for $F_1(c)$) isn't really a problem; computers don't care.

4

3. IMPLEMENTATION AND EXAMPLES



3.1. Implementation. A concise yet reasonably efficient implementation is worth a thousand formulas. It completely removes ambiguities, it tests the theories, and it allows for experimentation. Hence our next task is to implement. The section that follows was generated from a Mathematica [Wo] notebook which is available at [BV3, Theta.nb]. A second implementation of Θ , using Python and SageMath (<https://www.sagemath.org/>) is available at <https://www.rolandvdv.nl/Theta/>.

We start by loading the package `KnotTheory` — it is only needed because it has many specific knots pre-defined. In this Section and in the next,  and  mean “human input” while  means “computer output”:



 `<< KnotTheory``  Loading KnotTheory` version of October 29, 2024, 10:29:52.1301.
Read more at <http://katlas.org/wiki/KnotTheory>.

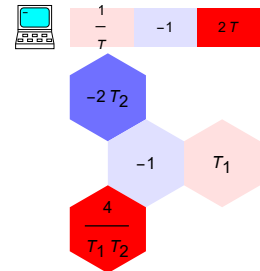
Next we quietly define the modules `Rot`, used to compute rotation numbers, and `PolyPlot`, used to plot polynomials as bar codes and as hexagonal QR codes. Neither is a part of the core of the computation of Θ , so neither is shown; yet we do show one usage example for each.

 `(* The definitions of Rot and PolyPlot are suppressed *)`


 `Rot[Mirror@Knot[3, 1]]`  `{{{1, 1, 4}, {1, 3, 6}, {1, 5, 2}}, {0, 0, 0, -1, 0, 0, 0}}`

We urge the reader to compare the above output with the knot diagram in Figure 2.1.


 `PolyPlot[{2 T - 1 + T-1, -1 + T1 - 2 T2 + 4 T1-1 T2-1},`
 `ImageSize → 100, Labeled → True]`







The definition of `CF` below is a technicality telling the computer how to best store polynomials in the $g_{\nu\alpha\beta}$'s such as F_1 and F_2 . The programs would run just the same without it, albeit a bit more slowly:


 `CF[\mathcal{E}] := Expand@Collect[\mathcal{E} , $\mathbf{g}_{__}$, \mathbf{F}] /. $\mathbf{F} \rightarrow \mathbf{Factor}$;`

Next, we decree that $T_3 = T_1 T_2$ and define the three “Feynman Diagram” polynomials F_1 , F_2 , and F_3 :



 `T3 = T1 T2;`

 $F_1[\{s_ , i_ , j_ \}] := CF[$
 $s \left(\frac{1}{2} - g_{3ii} + T_2^s g_{1ii} g_{2ji} - g_{1ii} g_{2jj} - (T_2^s - 1) g_{2ji} g_{3ii} + 2 g_{2jj} g_{3ii} - (1 - T_3^s) g_{2ji} g_{3ji} - \right.$
 $g_{2ii} g_{3jj} - T_2^s g_{2ji} g_{3jj} + g_{1ii} g_{3jj} +$
 $\left((T_1^s - 1) g_{1ji} (T_2^{s1} g_{2ji} - T_2^s g_{2jj} + T_2^s g_{3jj}) + \right.$
 $\left. (T_3^s - 1) g_{3ji} (1 - T_2^s g_{1ii} + g_{2ij} + (T_2^s - 2) g_{2jj} - (T_1^s - 1) (T_2^s + 1) g_{1ji}) \right) / (T_2^s - 1)]$

 $F_2[\{s0_ , i0_ , j0_ \}, \{s1_ , i1_ , j1_ \}] :=$
 $CF[s1 (T_1^{s0} - 1) (T_2^{s1} - 1)^{-1} (T_3^{s1} - 1) g_{1,j1,i0} g_{3,j0,i1}$
 $((T_2^{s0} g_{2,i1,i0} - g_{2,i1,j0}) - (T_2^{s0} g_{2,j1,i0} - g_{2,j1,j0}))]$


 $F_3[\varphi_ , k_] = \varphi g_{3kk} - \varphi / 2;$


Next comes the main program computing $\Theta(K)$. Fortunately, it matches perfectly with the mathematical description in Section 2. In line 1 below we use `Rot` to let X and φ be the crossings and rotation numbers of K . In addition we let n be the length of X , namely, the number of crossings in K and we let the starting value of A be the $(2n + 1) \times (2n + 1)$ identity matrix. Then in line 2, for each crossing in X we add to A a 2×2 block, in rows i and j and columns $i + 1$ and $j + 1$, as explain in Equation (1). In line 3 we compute the normalized Alexander polynomial Δ as in (2). In line 4 we let G be the inverse of A . In line 5 we declare what it means to evaluate, `ev`, a formula \mathcal{E} that may contain symbols of the form $g_{\nu\alpha\beta}$: each such symbol is to be replaced by the entry in position α, β of G , but with T replaced with T_ν . In line 6 we start computing θ by computing the first summand in (6), which in itself, is a sum over the crossings of the knot. In line 7 we add to θ the double sum corresponding to the second term in (6), and in line 8, we add the third summand of (6). Finally, line 9 outputs a pair: Δ , and the re-normalized version of θ .

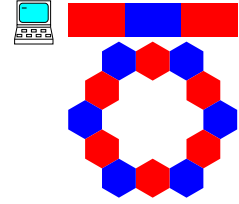
 $\Theta[K_] := \Theta[K] = \text{Module}[\{X, \varphi, n, A, \Delta, G, \text{ev}, \theta\},$
 $(* 1 *) \{X, \varphi\} = \text{Rot}[K]; n = \text{Length}[X]; A = \text{IdentityMatrix}[2 n + 1];$
 $(* 2 *) \text{Cases}[X, \{s_ , i_ , j_ \} \Rightarrow (A[\{i, j\}, \{i + 1, j + 1\}] += \begin{pmatrix} -T^s & T^s - 1 \\ 0 & -1 \end{pmatrix})];$
 $(* 3 *) \Delta = T^{(-\text{Total}[\varphi] - \text{Total}[X[\text{All}, 1]]) / 2} \text{Det}[A];$
 $(* 4 *) G = \text{Inverse}[A];$
 $(* 5 *) \text{ev}[\mathcal{E}_] := \text{Factor}[\mathcal{E} /. g_{\nu, \alpha, \beta} \Rightarrow (G[\alpha, \beta] /. T \rightarrow T_\nu)];$
 $(* 6 *) \theta = \text{ev}[\sum_{k=1}^n F_1[X[k]]];$
 $(* 7 *) \theta += \text{ev}[\sum_{k1=1}^n \sum_{k2=1}^n F_2[X[k1], X[k2]]];$
 $(* 8 *) \theta += \text{ev}[\sum_{k=1}^{12n} F_3[\varphi[k], k]];$
 $(* 9 *) \text{Factor}@\{\Delta, (\Delta /. T \rightarrow T_1) (\Delta /. T \rightarrow T_2) (\Delta /. T \rightarrow T_3) \theta\}$
 $];$

3.2. **Examples.** On to examples! Starting with the trefoil knot.

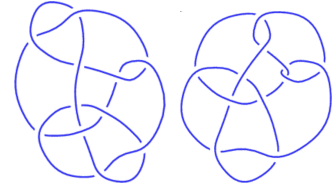
 `Expand[Theta[Knot[3, 1]]]`


 $\left\{ -1 + \frac{1}{T} + T, -\frac{1}{T_1^2} - T_1^2 - \frac{1}{T_2^2} - \frac{1}{T_1^2 T_2^2} + \frac{1}{T_1 T_2^2} + \frac{1}{T_1^2 T_2} + \frac{T_1}{T_2} + \frac{T_2}{T_1} + T_1^2 T_2 - T_2^2 + T_1 T_2^2 - T_1^2 T_2^2 \right\}$

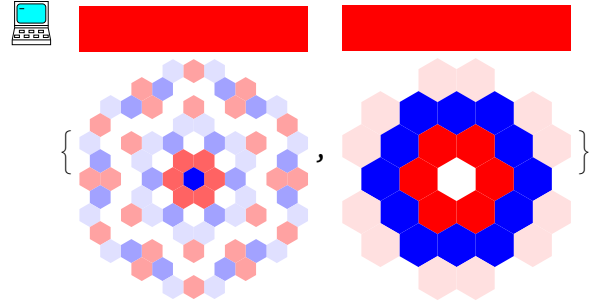
 `PolyPlot[Θ [Knot[3, 1]], ImageSize \rightarrow Tiny]`





Next are the Conway knot 11_{n34} and the Kinoshita-Terasaka knot 11_{n42} . The two are mutants and famously hard to separate: they both have $\Delta = 1$ (as evidenced by their one-bar Alexander bar codes below), and they have the same hyperbolic volume, HOMFLY-PT polynomial, and Khovanov homology. Yet their θ invariants are different. Note that the genus of the Conway knot is 3, while the genus of the Kinoshita-Terasaka knot is 2. This agrees with the apparent higher complexity of the QR code of the Conway polynomial and with Conjecture 16 below.

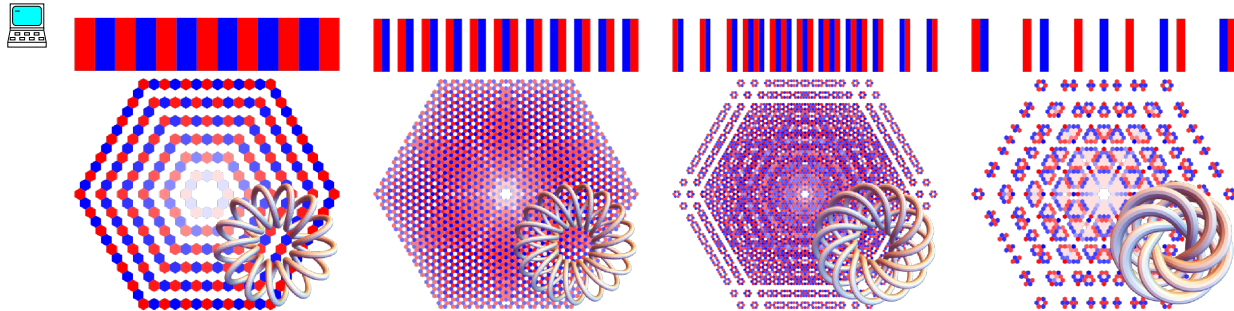


 `PolyPlot[Θ [Knot[#]], ImageSize \rightarrow 120] & /@ {"K11n34", "K11n42"}`




Torus knots have particularly nice-looking Θ invariants. Here are the torus knots $T_{13/2}$, $T_{17/3}$, $T_{13/5}$, and $T_{7/6}$:

 `ImageCompose[PolyPlot[Θ [TorusKnot @@ #], ImageSize \rightarrow 480],
 TubePlot[TorusKnot @@ #, ImageSize \rightarrow 240], {Right, Bottom}, {Right, Bottom}] & /@
{ {13, 2}, {17, 3}, {13, 5}, {7, 6} } // GraphicsRow`



The next line shows the computation time in seconds for the 132-crossing torus knot $T_{22/7}$ on a 2024 laptop, without actually showing the output. The output plot is in Figure 3.1.

 `AbsoluteTiming[Θ [TorusKnot[22, 7]]];]`

 {1020.73, Null}

We note that if T_1 and T_2 are assigned specific rational numbers and if the program for Θ is slightly modified so as to compute each G_ν separately (rather than computing G symbolically

```
ImageCompose[PolyPlot[Θ[TorusKnot[22, 7]], ImageSize → 720],  
TubePlot[TorusKnot[22, 7], ImageSize → 360], {Right, Bottom}, {Right, Bottom}]
```

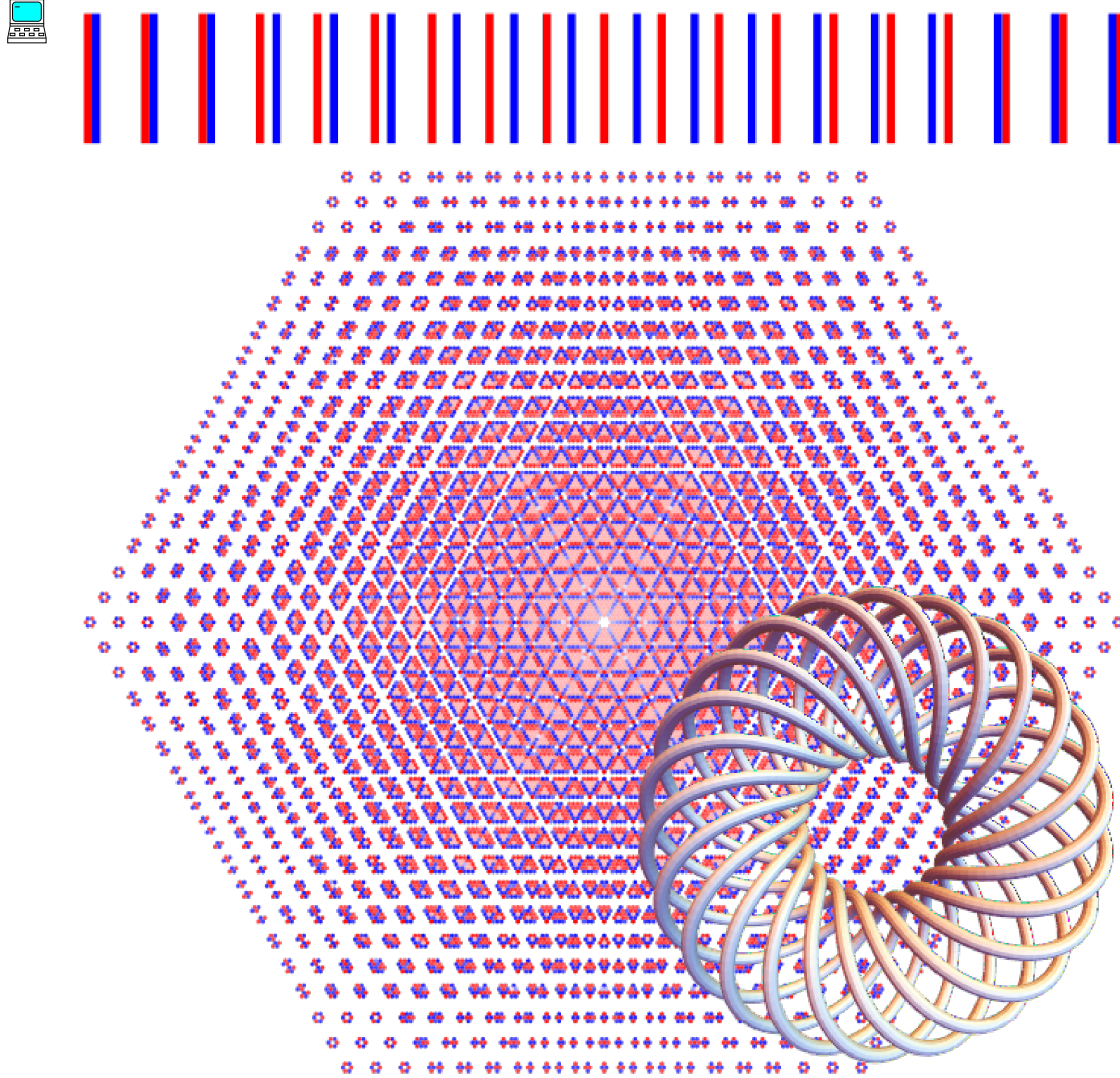


FIGURE 3.1. The 132-crossing torus knot $T_{22/7}$ and a plot of its Θ invariant

and then substituting $T \rightarrow T_\nu$), then the program becomes significantly more efficient, for inverting a numerical matrix is cheaper than inverting a symbolic matrix (but then one obtains numerical answers and the beauty and the topological significance (Section 5) are lost). The Mathematica notebook that accompanies this paper, [BV3, Theta.nb], contains the required modified program as well as a few computational examples. One finds that with $T_1 = 22/7$ and $T_2 = 21/13$, the invariant Θ can be computed for knots with 600 crossings, and that for knots with up to 15 crossings, its separation power remains the same.

If T_1 and T_2 are assigned approximate real values, say π and e computed to 100 decimal digits, then Θ can be computed on knots with 1,000 crossings and, for knots with up to 15 crossings it remains very strong. But approximate real numbers are a bit thorny. It is hard to know how far one needs to compute before deciding that two such numbers are equal,

and when two such numbers appear unequal, it is hard to tell if that is merely because they were computed differently and different roundings were applied. Thorns and snares are in the way of the perverse; He who guards his soul will be far from them (Proverbs 22:5)³.

4. PROOF OF INVARIANCE

Our proof of the invariance of θ (Theorem 1) is very similar, and uses many of the same pieces, as the proof of the invariance of ρ_1 in [BV1]. Thus at some places here we are briefer than at [BV1], and sadly, yet in the interest of saving space, we understate here the interpretation of $g_{\alpha\beta}$ as a “traffic function”.

Some Reidemeister moves create or lose an edge and to avoid the need for renumbering it is beneficial to also allow labelling the edges with non-consecutive labels. Hence we allow that, and write i^+ for the successor of the label i along the knot, and i^{++} for the successor of i^+ (these are $i + 1$ and $i + 2$ if the labelling is by consecutive integers). Also, by convention “1” will always refer to the label of the first edge, and “ $2n + 1$ ” will always refer to the label of the last. With this in mind, we have that $A = I + \sum_c A_c$, with A_c given by

$$\begin{array}{ccc} \begin{array}{c} j^+ \nearrow \quad \nearrow i^+ \\ i \searrow \quad \searrow j \\ s = +1 \end{array} & \begin{array}{c} i^+ \nearrow \quad \nearrow j^+ \\ j \searrow \quad \searrow i \\ s = -1 \end{array} & \longrightarrow \begin{array}{c|cc} A_c & \text{column } i^+ & \text{column } j^+ \\ \hline \text{row } i & -T^s & T^s - 1 \\ \text{row } j & 0 & -1 \end{array} \end{array} \quad (7)$$

Like in [BV1, Lemma 3], the equalities $AG = I$ and $GA = I$ imply that for any crossing $c = (s, i, j)$ in a knot diagram D , the Green function $G = (g_{\alpha\beta})$ of D satisfies the following “ g -rules”, with δ denoting the Kronecker delta:

$$g_{i\beta} = \delta_{i\beta} + T^s g_{i^+, \beta} + (1 - T^s) g_{j^+, \beta}, \quad g_{j\beta} = \delta_{j\beta} + g_{j^+, \beta}, \quad g_{2n+1, \beta} = \delta_{2n+1, \beta}, \quad (8)$$

$$g_{\alpha, i^+} = T^s g_{\alpha i} + \delta_{\alpha, i^+}, \quad g_{\alpha, j^+} = g_{\alpha j} + (1 - T^s) g_{\alpha i} + \delta_{\alpha, j^+}, \quad g_{\alpha, 1} = \delta_{\alpha, 1}. \quad (9)$$

Furthermore, the systems of equations (8) is equivalent to $AG = I$ and so it fully determines $g_{\alpha\beta}$, and likewise for the system (9), which is equivalent to $GA = I$.

Of course, the same g -rules also hold for $G_\nu = (g_{\nu\alpha\beta})$ for $\nu = 1, 2, 3$, except with T replaced with T_ν .

We also need a variant \tilde{g}_{ab} of $g_{\alpha\beta}$, defined whenever a and b are two distinct points on the edges of a knot diagram D , away from the crossings. If α is the edge on which a lies and β is the edge on which b lies, \tilde{g}_{ab} is defined as follows:

$$\tilde{g}_{ab} = \begin{cases} g_{\alpha\beta} & \text{if } \alpha \neq \beta, \\ g_{\alpha\beta} & \text{if } \alpha = \beta \text{ and } a < b \text{ relative to the orientation of the edge } \alpha = \beta, \\ g_{\alpha\beta} - 1 & \text{if } \alpha = \beta \text{ and } a > b \text{ relative to the orientation of the edge } \alpha = \beta. \end{cases} \quad (10)$$

Of course, we can define $\tilde{g}_{\nu ab}$ from $g_{\alpha\beta}$ in a similar way.

It is clear that g and \tilde{g} contain the same information and are easily computable from each other. The variant \tilde{g} is, strictly speaking, not a matrix and so g is a bit more suitable for computations. Yet \tilde{g} is a bit better behaved when we try to track, as below, the changes in g and \tilde{g} under Reidemeister moves. Reidemeister moves sometimes merge two edges into one or break an edge into two. In such cases the points a and b can be “pulled” along with the move so as to retain their ordering along the overall parametrization of the knot, yet mere

³ שומר נפשו ירחק.

edge labels lose this information. From the perspective of traffic functions, \tilde{g} is somewhat more natural than g , as it makes sense to inject traffic and to count traffic anywhere along an edge, provided the injection point and the counting point are distinct.

The following discussion and lemma further exemplify the advantage of \tilde{g} of g :

Discussion 5. We introduce “null vertices” as on the right into knot diagrams, whose only function (as we shall see) is to cut edges into parts that may carry different labels. When dealing with upright knot diagrams as in Figure 2.1, we only allow null vertices where the tangent to the knot is pointing up, so that the rotation numbers φ_k remain well defined on all edges. In the presence of null vertices the matrix A becomes a bit larger (by as many null vertices as were added to a knot diagram). The rule (7) for the creation of the matrix A gets an amendment for null vertices,

$$\begin{array}{c} j \quad k \\ \longrightarrow \bullet \longrightarrow \end{array} \longrightarrow \begin{array}{c|c} A_{nv} & \text{column } k \\ \hline \text{row } j & -1 \end{array},$$

and the summation for A , $A = I + \sum_c A_c + \sum_{nv} A_{nv}$ is extended to include summands for the null vertices. The matrix $G = A^{-1}$ and the function $g_{\alpha\beta}$ are defined as before. The g -rules of (8) and (9) get additions,

$$g_{j\beta} = \delta_{j\beta} + g_{k\beta}, \quad (11) \quad \text{and} \quad g_{\alpha k} = \delta_{\alpha k} + g_{\alpha j}, \quad (12)$$

and it remains true that the system of equations (8) \cup (11) (as well as (9) \cup (12)) fully determines $g_{\alpha\beta}$. The variant \tilde{g}_{ab} is also defined as before, except now a and b need to also be away from the null vertices.

Lemma 6. *Inserting a null vertex does not change \tilde{g}_{ab} provided it is inserted away from the points a and b .*⁴

Proof. Let D be an upright knot diagram having an edge labelled i and let D' be obtained from it by adding a null vertex within edge i , naming the two resulting half-edges j and k (in order). Let $g_{\alpha\beta}$ be the Green function for D , and similarly, $g'_{\alpha\beta}$ for D' . We claim that

$$g'_{\alpha\beta} = \begin{cases} \text{if } \beta = j & \text{if } \beta = k & \text{if } \beta \notin \{j, k\} \\ \begin{array}{ccc} g_{ii} & g_{ii} & g_{i\beta} \\ g_{ii} - 1 & g_{ii} & g_{i\beta} \\ g_{\alpha i} & g_{\alpha i} & g_{\alpha\beta} \end{array} & \begin{array}{l} \text{if } \alpha = j \\ \text{if } \alpha = k \\ \text{if } \alpha \notin \{j, k\} \end{array} \end{cases}$$

Indeed, all we have to do is to verify that the above-defined $g'_{\alpha\beta}$ satisfies all the g -rules (8) \cup (11), and that is easy. The lemma now follows easily from the definition of \tilde{g}' in Equation (10). \square

Remark 7. The statement of our Main Theorem, Theorem 1, does not change in the presence of null vertices: There are no “ F ” terms for those, and their only effect on the definition of Θ in Equation (6) is to change the edge labels that appear within c , c_1 , and c_2 , and within the F_3 sum.

The following theorem was not named in [BV1] yet it was stated there as the first part of the first proof of [BV1, Theorem 1].

⁴This statement does not make sense for $g_{\alpha\beta}$, as inserting a null vertex changes the dimensions of the matrix $G = (g_{\alpha\beta})$.

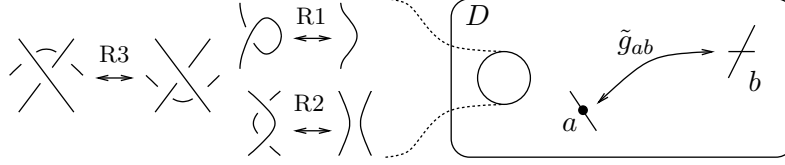


FIGURE 4.1. The modified Green function \tilde{g}_{ab} is invariant under Reidemeister moves performed away from where it is measured.

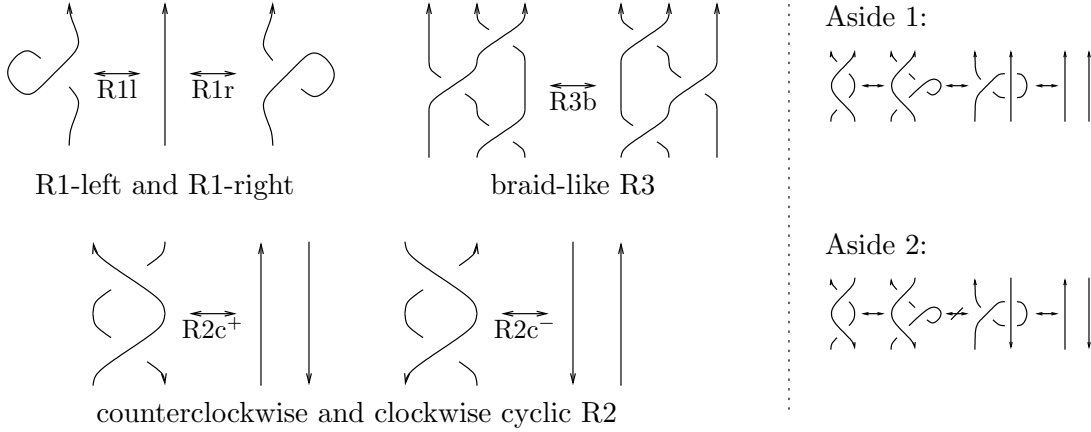


FIGURE 4.2. A generating set of oriented Reidemeister moves as in [Po2, Figure 6]. Aside 1: the braid-like R2b is not needed. Aside 2: yet R2b cannot replace R2c $^{\pm}$ because in the would-be proof, an unpostulated form of R3 is used (which in itself follows from R2c $^{\pm}$).

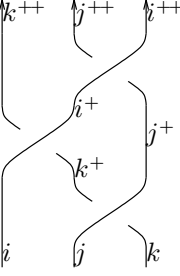
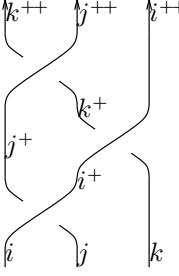
Theorem 8. *The variant Green function \tilde{g}_{ab} is a “relative invariant”, meaning that once points a and b are fixed within a knot diagram D , the value of \tilde{g}_{ab} does not change if Reidemeister moves are performed away from the points a and b (an illustration appears in Figure 4.1). It follows that the same is also true for $\tilde{g}_{\nu ab}$ for $\nu = 1, 2, 3$.*

We note that \tilde{g}_{ab} is nearly the same as $g_{\alpha\beta}$, if a is on α and b is on β . So Theorem 8 also says that $g_{\alpha\beta}$ is invariant under Reidemeister moves away from α and β , except for edge-renumbering issues and ± 1 contributions that arise if α and β correspond to edges that get merged or broken by the Reidemeister moves.

The proof of Theorem 8 is perhaps best understood in terms of the traffic function of Discussion 2: One simply needs to verify that for each of the Reidemeister moves, traffic entering the tangle diagram for the left hand side of the move exits it in the same manner as traffic entering the tangle diagram for the right hand side of the move, and each of these verifications, as explained in [BV1, BN3, BN6], is very easy. Yet that proof is a bit informal, so we opt here to give a fully formal proof along the lines of the first halves of [BV1, Propositions 7-9].

Proof of Theorem 8. We need to know how the Green function $g_{\alpha\beta}$ changes under the orientation-sensitive Reidemeister moves of Figure 4.2 (note that the $g_{\alpha\beta}$ do not see the rotation numbers and don’t care if a knot diagram is upright in the sense of Figure 2.1).

We start with R3b. Below are the two sides of the move, along with the g -rules of type (8) corresponding to the crossings within, written with the assumption that β isn't in $\{i^+, j^+, k^+\}$, so several of the Kronecker deltas can be ignored. We use g for the Green function at the left-hand side of R3b, and g' for the right-hand side:

	$\begin{aligned} g_{i^+, \beta} &= T g_{i^{++}, \beta} + (1-T) g_{j^{++}, \beta} \\ g_{j^+, \beta} &= g_{j^{++}, \beta} \\ g_{i, \beta} &= \delta_{i\beta} + T g_{i^+, \beta} + (1-T) g_{k^{++}, \beta} \\ g_{k^+, \beta} &= g_{k^{++}, \beta} \\ g_{j, \beta} &= \delta_{j\beta} + T g_{j^+, \beta} + (1-T) g_{k^+, \beta} \\ g_{k, \beta} &= \delta_{k\beta} + g_{k^+, \beta} \end{aligned}$		$\begin{aligned} g'_{j^+, \beta} &= T g'_{j^{++}, \beta} + (1-T) g'_{k^{++}, \beta} \\ g'_{k^+, \beta} &= g'_{k^{++}, \beta} \\ g'_{i^+, \beta} &= T g'_{i^{++}, \beta} + (1-T) g'_{k^+, \beta} \\ g'_{k, \beta} &= \delta_{k\beta} + g'_{k^+, \beta} \\ g'_{i, \beta} &= \delta_{i\beta} + T g'_{i^+, \beta} + (1-T) g'_{j^+, \beta} \\ g'_{j, \beta} &= \delta_{j\beta} + g'_{j^+, \beta} \end{aligned}$
...
further crossings	further g -rules	further crossings	further g' -rules

Recall that along with the further g -rules and/or g' -rules corresponding to all the non-moving knot crossings, these rules fully determine $g_{\alpha\beta}$ and $g'_{\alpha\beta}$ for $\beta \notin \{i^+, j^+, k^+\}$.

A routine computation (eliminating $g_{i^+, \beta}$, $g_{j^+, \beta}$, and $g_{k^+, \beta}$) shows that the first system of 6 equations is equivalent to the following system of 6 equations:

$$g_{i, \beta} = \delta_{i\beta} + T^2 g_{i^{++}, \beta} + T(1-T) g_{j^{++}, \beta} + (1-T) g_{k^{++}, \beta}, \quad (13)$$

$$\begin{aligned} g_{j, \beta} &= \delta_{j\beta} + T g_{j^{++}, \beta} + (1-T) g_{k^{++}, \beta}, & g_{k, \beta} &= \delta_{k\beta} + g_{k^{++}, \beta}, \\ g_{i^+, \beta} &= T g_{i^{++}, \beta} + (1-T) g_{j^{++}, \beta}, & g_{j^+, \beta} &= g_{j^{++}, \beta}, & g_{k^+, \beta} &= g_{k^{++}, \beta}. \end{aligned} \quad (14)$$

In this system the indices i^+ , j^+ and k^+ do not appear in (13) or in the further g -rules corresponding to the further crossings. Hence for the purpose of determining $g_{\alpha\beta}$ with $\alpha, \beta \notin \{i^+, j^+, k^+\}$, Equations (14) can be ignored.

Similarly eliminating $g'_{i^+, \beta}$, $g'_{j^+, \beta}$, and $g'_{k^+, \beta}$ from the second set of equations, we find that it is equivalent to

$$\begin{aligned} g'_{i, \beta} &= \delta_{i\beta} + T^2 g'_{i^{++}, \beta} + T(1-T) g'_{j^{++}, \beta} + (1-T) g'_{k^{++}, \beta}, \\ g'_{j, \beta} &= \delta_{j\beta} + T g'_{j^{++}, \beta} + (1-T) g'_{k^{++}, \beta}, & g'_{k, \beta} &= \delta_{k\beta} + g'_{k^{++}, \beta}, \end{aligned} \quad (15)$$

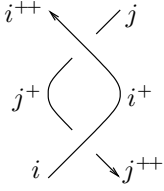
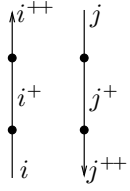
$$g'_{i^+, \beta} = T g'_{i^{++}, \beta} + (1-T) g'_{k^{++}, \beta}, \quad g'_{j^+, \beta} = T g'_{j^{++}, \beta} + (1-T) g'_{k^{++}, \beta}, \quad g'_{k^+, \beta} = g'_{k^{++}, \beta}. \quad (16)$$

Using the same logic as before, for the purpose of determining $g'_{\alpha\beta}$ with $\alpha, \beta \notin \{i^+, j^+, k^+\}$, Equations (16) can be ignored.

But now we compare the unignored equations, (13) and (15), and find that they are exactly the same, except with $g \leftrightarrow g'$, and the same is true for the further g -rules and/or g' -rules coming from the further crossings. Hence so long as $\alpha, \beta \notin \{i^+, j^+, k^+\}$, we have that $g_{\alpha\beta} = g'_{\alpha\beta}$. In the case of the R3b move no edges merge or break up, and hence this implies that $\tilde{g}_{ab} = \tilde{g}'_{ab}$ so long as a and b are away from the move.

Next we deal with the case of R2c⁺. We use the privileges afforded to us by Lemma 6 to insert 4 null vertices into the right-hand-side of the move, and like in the case of R3b, we start with pictures annotated with the relevant type (8) and (11) g -rules, written with the

assumption that $\beta \notin \{i^+, j^+\}$:

	$g_{i^+, \beta} = T g_{i^{++}, \beta} + (1 - T) g_{j^+, \beta}$ $g_{j, \beta} = \delta_{j, \beta} + g_{j^+, \beta}$ $g_{i, \beta} = \delta_{i, \beta} + T^{-1} g_{i^+, \beta} + (1 - T^{-1}) g_{j^{++}, \beta}$ $g_{j^+, \beta} = g_{j^{++}, \beta}$		$g'_{i, \beta} = \delta_{i, \beta} + g'_{i^+, \beta}$ $g'_{j^+, \beta} = g'_{j^{++}, \beta}$ $g'_{i^+, \beta} = g'_{i^{++}, \beta}$ $g'_{j, \beta} = \delta_{j, \beta} + g'_{j^+, \beta}$
...
further crossings	further g-rules	further crossings	further g'-rules

As in the case of R3b, we eliminate $g_{i^+, \beta}$ and $g_{j^+, \beta}$ from the equations for the left hand side, and find that for the purpose of determining $g_{\alpha\beta}$ with $\beta \notin \{i^+, j^+\}$, they are equivalent to the equations

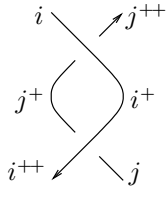
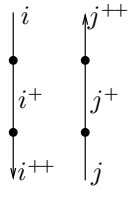
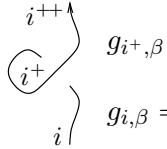
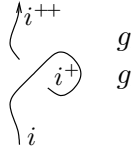
$$g_{i, \beta} = \delta_{i, \beta} + g_{i^{++}, \beta} \quad \text{and} \quad g_{j, \beta} = \delta_{j, \beta} + g_{j^{++}, \beta}.$$

Likewise, the right hand side is clearly equivalent to

$$g'_{i, \beta} = \delta_{i, \beta} + g'_{i^{++}, \beta} \quad \text{and} \quad g'_{j, \beta} = \delta_{j, \beta} + g'_{j^{++}, \beta},$$

and as in the case of R3b, this establishes the invariance of \tilde{g}_{ab} under R2c moves.

For the remaining moves, R2c⁻, R1l, and R1r, we merely display the g -rules and leave it to the readers to verify that when the edges i^+ and/or j^+ are eliminated, the left hand sides become equivalent to the right hand sides:

	$g_{i, \beta} = \delta_{i, \beta} + T g_{i^+, \beta} + (1 - T) g_{j^{++}, \beta}$ $g_{j^+, \beta} = g_{j^{++}, \beta}$ $g_{i^+, \beta} = T^{-1} g_{i^{++}, \beta} + (1 - T^{-1}) g_{j^+, \beta}$ $g_{j, \beta} = \delta_{j, \beta} + g_{j^+, \beta}$		$g'_{i, \beta} = \delta_{i, \beta} + g'_{i^+, \beta}$ $g'_{j^+, \beta} = g'_{j^{++}, \beta}$ $g'_{i^+, \beta} = g'_{i^{++}, \beta}$ $g'_{j, \beta} = \delta_{j, \beta} + g'_{j^+, \beta}$
	$g_{i^+, \beta} = T g_{i^{++}, \beta} + (1 - T) g_{i^+, \beta}$ $g_{i, \beta} = \delta_{i, \beta} + g_{i^+, \beta}$		$g''_{i^+, \beta} = g''_{i^{++}, \beta}$ $g''_{i, \beta} = \delta_{i, \beta} + T g''_{i^+, \beta} + (1 - T) g''_{i^{++}, \beta}$

8

We can now move on to the main part of the proof of our Main Theorem, Theorem 1. We need to show the invariance of θ under the “upright Reidemeister” moves of Figure 4.3.

Proposition 9. *The moves in Figure 4.3 are sufficient. If two upright knot diagrams (with null vertices) represent the same knot, they can be connected by a sequence of moves as in the figure.*

Proof Sketch. There is an obvious well-defined map

$$\frac{\text{upright knot diagrams}}{\text{relations as in Figure 4.3}} \longrightarrow \frac{\text{oriented knot diagrams}}{\text{relations as in Figure 4.2}}$$

We merely have to construct an inverse to that map. To do that we merely have to choose how to turn each crossing in an oriented knot diagram to be upright. The different ways of doing so differ by instances of the Sw relation (if deeper spirals need to be swirled away, null vertices may be inserted using NV and the spirals can be undone one rotation at a time). A more detailed version of the proof is in [BVH]. □

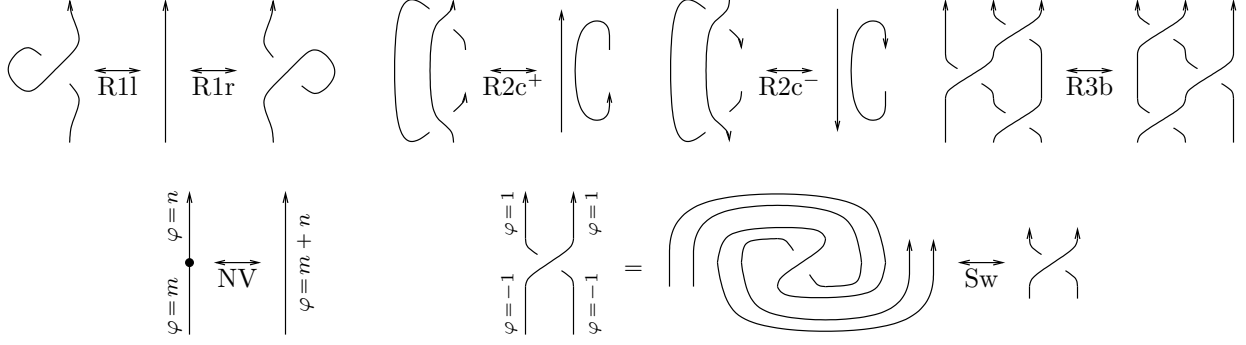


FIGURE 4.3. The upright Reidemeister moves: The R1 and R3 moves are already upright and remain the same as in Figure 4.2. The crossings in the R2 moves of Figure 4.2 are rotated to be upright. We also need two further moves: The null vertex move NV for adding and removing null vertices, and the swirl move Sw which then implies that any two ways of turning a crossing upright are the same. We sometimes indicate rotation numbers symbolically rather than using complicated spirals.

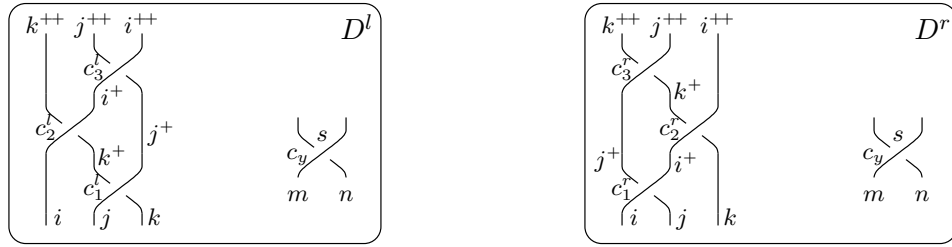


FIGURE 4.4. The two sides D^l and D^r of the R3b move. The left side D^l consists of 3 distinguished crossings $c_1^l = (1, j, k)$, $c_2^l = (1, i, k^+)$, $c_3^l = (1, i^+, j^+)$ and a collection of further crossings $c_y = (s, m, n) \in Y$, where Y is the set of crossings not participating in the R3b move. The right side D^r consists of $c_1^r = (1, i, j)$, $c_2^r = (1, i^+, k)$, $c_3^r = (1, j^+, k^+)$ and the same set Y of further crossings c_y .

Proposition 10. *The quantity θ is invariant under R3b.*

Proof. Let D_l and D_r be two knot diagrams that differ only by an R3b move, and label their relevant edges and crossings as in Figure 4.4. Let $g_{\nu\alpha\beta}^l$ and $g_{\nu\alpha\beta}^r$ be their corresponding Green functions. Let $F_1^l(c)$, $F_2^l(c_0, c_1)$ and $F_3^l(\varphi, k)$ be defined from $g_{\nu\alpha\beta}^l$ as in (3)–(5), and similarly make F_1^r , F_2^r and F_3^r using $g_{\nu\alpha\beta}^r$.

By the invariance of the Alexander polynomial, the pre-factor $\Delta_1\Delta_2\Delta_3$ is the same for $\theta(D^l)$ and for $\theta(D^r)$ (see Equation (6)). By Theorem 8, $g_{\nu\alpha\beta}^l = g_{\nu\alpha\beta}^r$ so long as $\alpha, \beta \notin \{i^+, j^+, k^+\}$. And so the only terms that may differ in $\theta(D^h)$ between $h = l$ and $h = r$ are the terms

$$A^h = \sum_{c \in \{c_1^h, c_2^h, c_3^h\}} F_1^h(c) + \sum_{c_0, c_1 \in \{c_1^h, c_2^h, c_3^h\}} F_2^h(c_0, c_1), \quad B^h = \sum_{c_0 \in \{c_1^h, c_2^h, c_3^h\}, c_y \in Y} F_2^h(c_0, c_y), \quad \text{and} \quad C^h = \sum_{c_1 \in \{c_1^h, c_2^h, c_3^h\}, c_y \in Y} F_2^h(c_y, c_1). \quad (17)$$

We claim that $A^l = A^r$, $B^l = B^r$, and $C^l = C^r$.

To show that $A^l = A^r$, we need to compare polynomials in $g_{\nu\alpha\beta}^l$ with polynomials in $g_{\nu\alpha\beta}^r$ in which α and β may belong to the set $\{i^+, j^+, k^+\}$ on which it may be that $g^l \neq g^r$. Fortunately the g -rules of Equations (8) and (9) allow us to rewrite the offending g 's, namely the ones with subscripts in $\{i^+, j^+, k^+\}$, in terms of other g 's whose subscripts are in $\{i, j, k, i^{++}, j^{++}, k^{++}\}$, where $g^l = g^r$. So it is enough to show that

$$\text{under } g^l = g^r, \quad A^l /. (\text{the } g\text{-rules for } c_1^l, c_2^l, c_3^l) = A^r /. (\text{the } g\text{-rules for } c_1^r, c_2^r, c_3^r), \quad (18)$$

where the symbol $/.$ means “apply the rules”. This is a finite computation that can in principle be carried out by hand. But each A^h is a sum of $3 + 9 = 12$ polynomials in the g^l 's or the g^r 's, these polynomials are rather unpleasant (see (3) and (4)), and applying the relevant g -rules adds a bit further to the complexity. Luckily, we can delegate this pages-long calculation to an entity that works accurately and doesn't complain.

First, we implement the Kronecker δ -function, the g -rules for a crossing (s, i, j) , and the g -rules for a list of crossings X :

```

δi,j := If[i === j, 1, 0];
gRules[{s_, i_, j_}] := {
  gv,jβ → gv,j+β + δjβ, gv,iβ → Tvs gv,i+β + (1 - Tvs) gv,j+β + δiβ,
  gv,αi+ → Tvs gv,αi + δαi+, gv,αj+ → gv,αj + (1 - Tvs) gv,αi + δαj+
};
gRules[X__List] := Union @@ Table[gRules[c], {c, {X}}]

```

We then let $X1$ be the three crossings in the left-hand-side of the R3b move, as in Figure 4.4, we let $A1$ be the A^l term of (17), and we let lhs be the result of applying the g -rules for the crossings in $X1$ to $A1$. We print only a “Short” version of lhs because the full thing would cover about 2.5 pages:

```

X1 = {{1, j, k}, {1, i, k+}, {1, i+, j+}};
A1 = Sum[F1[c], {c, X1}] + Sum[F2[c0, c1], {c0, X1}, {c1, X1}];
lhs = Simplify[A1 /. gRules @@ X1];
Short[lhs, 5]

```

$$\begin{aligned}
& -\frac{1}{2(1-T_2)} \left(3 - 3T_2 + \ll 129 \gg + \right. \\
& \quad 2(1-T_2) \left(1 + T_2 (T_2 g_{2, \ll 1 \gg^+, i} - (-1 + T_2) g_{2, \ll 1 \gg, i}) - (-1 + T_2) g_{2, (k^+)^+, i} \right) \\
& \quad \left. (1 + (1 - T_1 T_2) g_{3, (k^+)^+, j} + g_{3, (k^+)^+, k}) \right)
\end{aligned}$$

We do the same for A^r , except this time, without printing at all:

```

Xr = {{1, i, j}, {1, i+, k}, {1, j+, k+}};
Ar = Sum[F1[c], {c, Xr}] + Sum[F2[c0, c1], {c0, Xr}, {c1, Xr}];
rhs = Simplify[Ar /. gRules @@ Xr];

```

We then compare lhs with rhs . The output, `True`, tells us that we have proven (18):

```

Simplify[lhs == rhs]

```

 True

We show that $B^l = B^r$ by following exactly the same procedure. Note that we ignore the summation over c_y and instead treat c_y as a fixed crossing (s, m, n) . If an equality is proven for every fixed c_y , it is of course also proven for the sum over $c_y \in Y$.

```

-- lhs = Sum[F2[c0, {s, m, n}], {c0, Xl}] //. gRules @@ Xl;
-- rhs = Sum[F2[c0, {s, m, n}], {c0, Xr}] //. gRules @@ Xr;
Simplify[lhs == rhs]

```

True

Similarly we prove that $C^l = C^r$, and this concludes the proof of Proposition 10.

```

-- lhs = Sum[F2[{s, m, n}, c1], {c1, Xl}] //. gRules @@ Xl;
-- rhs = Sum[F2[{s, m, n}, c1], {c1, Xr}] //. gRules @@ Xr;
Simplify[lhs == rhs]

```

True

10

Remark 11. The computations above were carried out for generic $g_{\nu\alpha\beta}$ and for a generic $c_y = (s, m, n)$; namely, without specifying the knot diagrams in full, and hence without assigning specific values to $g_{\nu\alpha\beta}$, and without specifying m and n . Under these conditions the three parts of (17) cannot mix (namely, terms from, say, A^h cannot cancel terms in B^h or C^h), and so it would have been enough to show that $E^l = E^r$, where E^h combines A^h and B^h and C^h (and a few harmless further terms) by adding c_y to the summation corresponding to A^h :

$$E^h = \sum_{c \in \{c_1^h, c_2^h, c_3^h, c_y\}} F_1^h(c) + \sum_{c_0, c_1 \in \{c_1^h, c_2^h, c_3^h, c_y\}} F_2^h(c_0, c_1).$$

But that's a simpler computation:

```

-- ESum[X_] := (Sum[F1[c], {c, X}] + Sum[F2[c0, c1], {c0, X}, {c1, X}]) //. gRules @@ X;
-- Xl = {{1, j, k}, {1, i, k+}, {1, i+, j+}};
-- Xr = {{1, i, j}, {1, i+, k}, {1, j+, k+}};
Simplify[ESum[Append[Xl, {s, m, n}]] == ESum[Append[Xr, {s, m, n}]]]

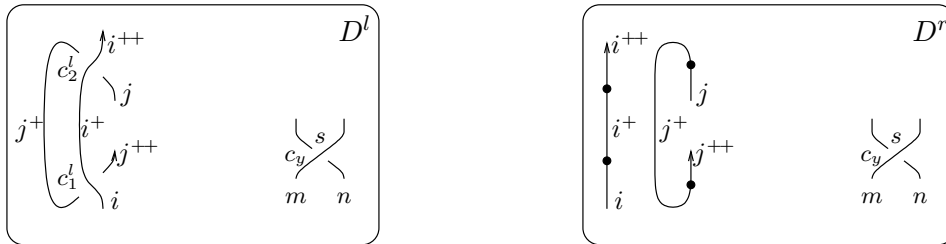
```

True

11

Proposition 12. *The quantity θ is invariant under the upright $R2c^+$ and $R2c^-$.*

Proof. For $R2c^+$ we follow the same logic as in the proof of Proposition 10, as simplified by Remark 11. We start with the figure that replaces Figure 4.4 (note the null vertices in D^r and their minimal effect as in Lemma 6 and Remark 7):



As in Remark 11, we let E^l and E^r be the sums corresponding to the diagrams D^l and D^r above:

$$E^l = \sum_{c \in \{c_1^l, c_2^l, c_y\}} F_1^l(c) + \sum_{c_0, c_1 \in \{c_1^l, c_2^l, c_y\}} F_2^l(c_0, c_1) + F_3^l(j^+) |_{\varphi_{j^+}=1}, \quad E^r = F_1^r(c_y) + F_2^r(c_y, c_y) + F_3^r(j^+) |_{\varphi_{j^+}=1}.$$

We need to show that $E^l = E^r$ after all relevant g -rules are applied to both sides.

To compute these E sums we first have to extend the **ESum** routine to accept also a list R of pairs (φ, k) of the form (rotation number, edge label):

```

-- ESum[X_, R_] :=
-- (Sum[F1[c], {c, X}] + Sum[F2[c0, c1], {c0, X}, {c1, X}] + Sum[F3@@r, {r, R}]) //.
-- gRules@@X;

```

We then compute E^l (and apply the relevant g -rules) by calling **ESum** with crossings $(-1, i, j^+)$, $(1, i^+, j)$, and (s, m, n) , and a rotation number of 1 on edge j^+ :

```

-- E1 = Simplify[ESum[{{-1, i, j^+}, {1, i^+, j}, {s, m, n}}, {{1, j^+}}]];
-- Short[E1, 5]

```

$$\begin{aligned}
& -\frac{1}{2(-1 + T_2^5)} \left((1 + s + 2s(T_1 T_2)^s g_{3,m^+,m} + \ll 11 \gg + 2g_{3,(j^+)^+,j} - \right. \\
& \quad \left. T_2^s (1 + s - 2s g_{1,n^+,m} g_{2,n^+,m} + 2s g_{2,n^+,n} + \ll 28 \gg + 2s g_{2,m^+,m} (1 + g_{3,n^+,n}) + 2g_{3,(j^+)^+,j}) \right)
\end{aligned}$$

The computation of E^r is simpler, as it only involves the generic (s, m, n) and the rotation $(1, j^+)$. We implement the g -rules for null vertices as in Equations (11) and (12), compute E^r , and then compare E^l with E^r to conclude the invariance under $R2c^+$:

```

-- gRules[j_] := {g_{v_-,j,\beta} \Rightarrow \delta_{j,\beta} + g_{v_-,j^+,\beta}, g_{v_-, \alpha_-, j^+} \Rightarrow \delta_{\alpha, j^+} + g_{v_-, \alpha, j}}
-- Er = ESum[{{s, m, n}}, {{1, j^+}}] //. (Union@@gRules /@ {i, i^+, j, j^+});
-- Simplify[E1 == Er]

```

True

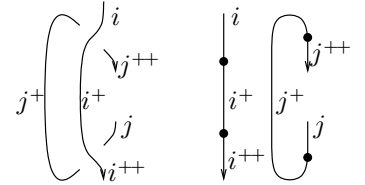
For $R2c^-$ we allow ourselves to be even more condensed:

```

-- E1 = ESum[{{1, i, j^+}, {-1, i^+, j}, {s, m, n}}, {{-1, j^+}}];
-- Er = ESum[{{s, m, n}}, {{-1, j^+}}] //.
-- (Union@@gRules /@ {i, i^+, j, j^+});
-- Simplify[Er == E1]

```

True



12

Proposition 13. *The quantity θ is invariant under $R1l$ and $R1r$.*

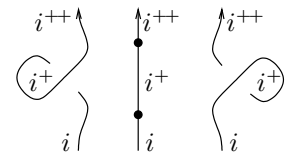
Proof. We aim to use the same approach and conventions as in the previous two proofs but hit a minor snag. The g -rules for $R1l$ include


$$g_{i+\beta} = \delta_{i+\beta} + T g_{i^{++},\beta} + (1 - T) g_{i^+, \beta} \quad \text{and} \quad g_{\alpha, i^+} = g_{\alpha i} + (1 - T) g_{\alpha i^+} + \delta_{\alpha, i^+},$$

and if these are implemented as simple left to right replacement rules, they lead to infinite recursion. Fortunately, these rules can be rewritten in the form

$$g_{i+\beta} = T^{-1} \delta_{i+\beta} + g_{i^{++}, \beta} \quad \text{and} \quad g_{\alpha, i^+} = T^{-1} g_{\alpha i} + T^{-1} \delta_{\alpha, i^+},$$

which makes perfectly valid replacement rules. We thus redefine:





```

gRules[{1, i+, i}] = {
  gviβ- ⇔ gvi+β + δiβ, gvi+β- ⇔ gv(i+)+β + Tv-1δi+β,
  gvα-(i+)+ ⇔ Tvgvαi+ + δα(i+)+, gvα-i+ ⇔ Tv-1gvαi + Tv-1δαi+
};

```

shorten

The same issue does not arise for R1r (!), and thus the following lines conclude the proof:

```

E1 = ESum[{1, i+, i}, {s, m, n}, {1, i+}}];
Em = ESum[{s, m, n}];
Er = ESum[{1, i, i+}, {s, m, n}, {-1, i+}}];
Simplify[E1 == Em == Er]

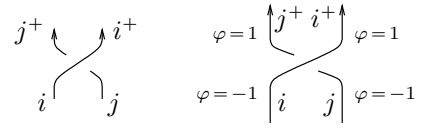
```

 True

13

Proposition 14. *The quantity θ is invariant under Sw.*

Proof. This one is routine:



```

E1 = ESum[{1, i, j}, {s, m, n}];
Er = ESum[{1, i, j}, {s, m, n}, {-1, i}, {-1, j}, {1, i+}, {1, j+}}];
Simplify[E1 == Er]

```

 True

14

Proposition 15. *The quantity θ is invariant under NV.*

Proof. Indeed, F_3 is linear in φ . □

We are now ready to complete the proof of the Main Theorem.

Proof of Theorem 1. The Main Theorem now follows from Propositions 9, 10, 12, 13, 14, and 15. □

5. STRONG AND MEANINGFUL

5.1. Strong. To illustrate the strength of Θ , Table 5.1 summarizes the separation powers of Θ and of some common knot invariants and combinations of those knot invariants on prime knots with up to 15 crossings (up to reflections and reversals).

In line 2 of the table we list the total number of tabulated knots with up to n crossings. For example, there are 313,230 prime knots up to reflections and reversals with at most 15 crossings. In the following lines we list the *separation deficits* on these knots, for different invariants or combinations of invariants. For example, in line 3 we can see that on knots with up to 10 crossings, the Alexander polynomial Δ has a separation deficit of 38: meaning, that it attains $249 - 38 = 211$ distinct values on the 249 knots with up to 10 crossings. For deficits, the smaller the better!⁵ Thus the deficit of 236,326 for Δ at $n \leq 15$ means that the Alexander polynomial is a rather weak invariant, in as much as separation power is concerned.

⁵This is not a political statement.

1	n	≤ 10	≤ 11	≤ 12	≤ 13	≤ 14	≤ 15
2	knots	249	801	2,977	12,965	59,937	313,230
3	Δ	(38)	(250)	(1,204)	(7,326)	(39,741)	(236,326)
4	σ	(108)	(356)	(1,525)	(7,736)	(40,101)	(230,592)
5	J	(7)	(70)	(482)	(3,434)	(21,250)	(138,591)
6	Kh	(6)	(65)	(452)	(3,226)	(19,754)	(127,261)
7	H	(2)	(31)	(222)	(1,839)	(11,251)	(73,892)
8	Vol	(~ 6)	(~ 25)	(~ 113)	($\sim 1,012$)	($\sim 6,353$)	($\sim 43,607$)
9	(Kh, H, Vol)	(~ 0)	(~ 14)	(~ 84)	(~ 911)	($\sim 5,917$)	($\sim 41,434$)
10	(Δ, ρ_1)	(0)	(14)	(95)	(959)	(6,253)	(42,914)
11	(Δ, ρ_1, ρ_2)	(0)	(14)	(84)	(911)	(5,926)	(41,469)
12	$(\rho_1, \rho_2, Kh, H, Vol)$	(0)	(~ 14)	(~ 84)	(~ 911)	($\sim 5,916$)	($\sim 41,432$)
13	Θ	(0)	(3)	(19)	(194)	(1,118)	(6,758)
14	(Θ, ρ_2)	(0)	(3)	(10)	(169)	(982)	(6,341)
15	(Θ, σ)	(0)	(3)	(19)	(194)	(1,118)	(6,758)
16	(Θ, Kh)	(0)	(3)	(18)	(185)	(1,062)	(6,555)
17	(Θ, H)	(0)	(3)	(18)	(185)	(1,064)	(6,563)
18	(Θ, Vol)	(0)	(~ 3)	(~ 10)	(~ 169)	(~ 973)	($\sim 6,308$)
19	$(\Theta, \rho_2, Kh, H, Vol)$	(0)	(~ 3)	(~ 10)	(~ 169)	(~ 972)	($\sim 6,304$)

TABLE 5.1. The separation powers of some knot invariants and combinations of knot invariants (in lines 3–19, smaller numbers are better). The data in this table was assembled by [BV3, Stats.nb].

In line 4 we show the deficits for the Levine-Tristram signature [Le, Tr, Co] as computed by the program in [BN4]. We were surprised to find that for knots with up to 15 crossings these deficits are smaller than those of Δ .

Line 5 shows the deficits for the Jones polynomial J . It is better than Δ , and better than Δ and σ taken together (deficits not shown) but still rather weak. Line 6 shows the deficits for Khovanov homology Kh . They are only a bit lower than those of J . On line 7, the HOMFLY-PT polynomial H is noticeably better.

On line 8 we consider the hyperbolic volume Vol of the knot complement, as computed by SnapPy [CDGW]. We computed volumes using SnapPy's `high_precision` flag, which makes SnapPy compute to roughly 63 decimal digits, and then truncated the results to 58 decimal digits to account for possible round-off errors within the last few digits. But then we are unsure if we computed enough. . . . Hence the uncertainty symbols “ \sim ” on some of the results here and in the other lines that contain Vol . This said, Vol seems to be the champion so far.

Line 9 is “everything so far, taken together”. Note that Kh dominates J and H dominates both Δ and J , so there's no point adding Δ and/or J into the mix. We note that adding σ to the triple (Kh, H, Vol) , or even to the pair (Kh, Vol) , does not improve the results; namely, for knots with up to 15 crossings the pair (Kh, Vol) dominates σ , even though each of Kh and Vol does not dominate σ and the discrepancies start already at 11 crossings. We don't know if this means anything.

On line 10, the Rozansky-Overbay invariant ρ_1 [Roz1, Roz2, Roz3, Ov], also discussed by us in [BV1], does somewhat better. Note that the computation of Δ is a part of the computation of ρ_1 , so we always take them together. In line 11 we add ρ_2 [BN3] to make the results yet a bit better.

Line 12 is “everything before Θ ”.

Line 13 makes our case that Θ is strong — the deficit here, for knots with up to 15 crossings, is about a sixth of the deficit in line 12!

Line 14 reinforces our case by just a bit: note that it makes sense to bundle ρ_2 along with Θ , for their computations are very similar. Note also that Conjecture 21 below means that it is pointless to consider (Θ, ρ_1) .

Line 15 shows that for knots with up to 15 crossings, Θ dominates σ . We don’t know if this persists.

Lines 16 through 18 show that at crossing number ≤ 15 and in the presence of Θ , and especially in the presence of both Θ and ρ_2 , it is pointless to also consider H or Kh , and only mildly useful to also consider Vol . Line 19 shows that once Vol has been added to Θ , the other invariants contribute almost nothing.

We note that of all the invariants considered above, the only one known to (sometimes) detect knot mutation is Θ (see Section 3.2).

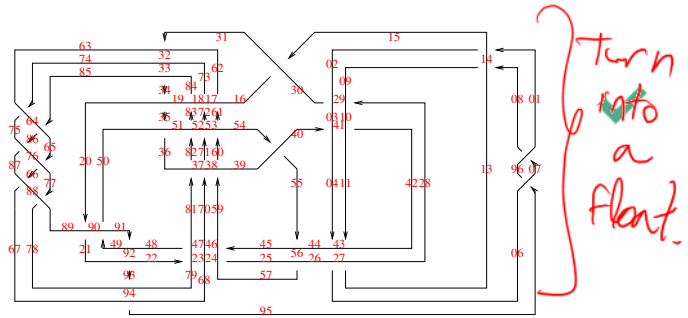
We also note that the V_n polynomials of Garoufalidis and Kashaev [GK], and in particular V_2 [GL] share many properties with Θ and are stronger than Θ on knots with up to 15 crossings. But they are not nearly as computable on large knots. It would be very interesting to explore the relationship between the V_n ’s and Θ .

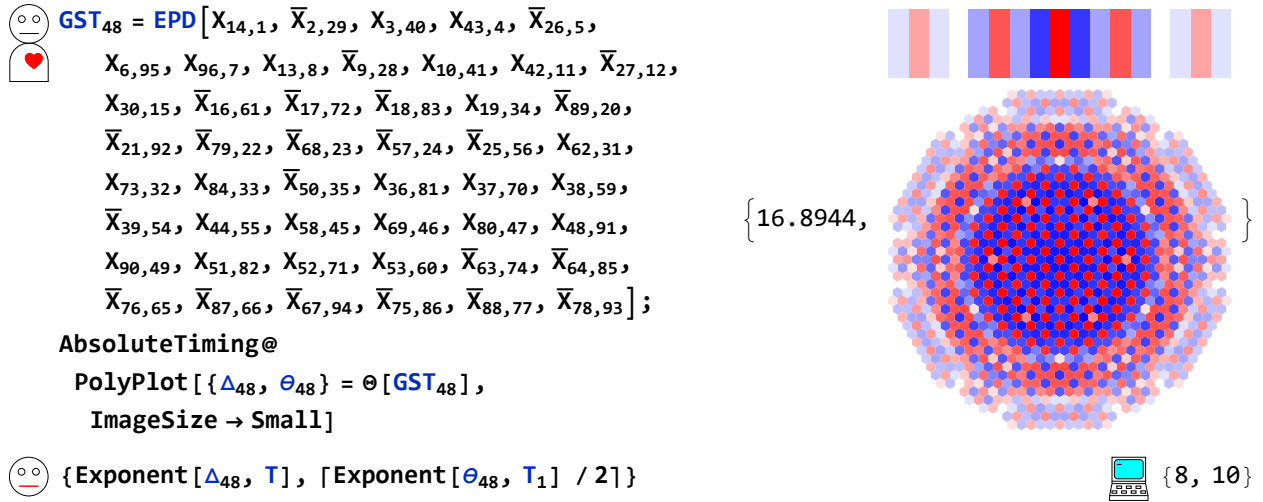
5.2. Meaningful. Many knot polynomials have some separation power, some more and some less, yet they seem to “see” almost no other topological properties of knots. The greatest exception is the Alexander polynomial, which despite having rather weak separation powers, gives a genus bound, a fiberedness condition, and a ribbon condition. The definition of θ is in some sense “near” the definition of Δ , and one may hope that θ will share some of the good topological properties of Δ .

5.2.1. The Knot Genus. With significant computational and theoretical (see also Discussion 23 and Comment 26 below) evidence we believe the following to be true:

Conjecture 16. *Let K be a knot and $g(K)$ the genus of K . Then $\deg_{T_1} \theta(K) \leq 2g(K)$.*

Using the available genus data in KnotInfo [LM] we have verified this conjecture for all knots with up to 13 crossings (see [BV3, KnotGenus.nb]). The example of the Conway knot and the Kinoshita-Terasaka knot in Section 3.2 shows that the bound in Conjecture 16 can be stronger than the bound $\deg_T \Delta(K) \leq g(K)$ coming from the Alexander polynomial. Another such example is the 48-crossing Gompf-Scharlemann-Thompson GST_{48} knot [GST], shown on the right. Here’s the relevant computation, with $X_{14,1}$ (say) meaning “the crossing (1, 14, 1)” and $\bar{X}_{2,29}$ (say) meaning “ $(-1, 2, 29)$ ”:





Thus θ gives a better lower bound on the genus of GST_{48} , 10, then the lower bound coming from Δ , which is 8. Seeing that GST_{48} may be a counter-example to the ribbon-slice conjecture [GST], we are happy to have learned more about it. Also see Dream 34 below.

The hexagonal QR code of large knots is often a clear hexagon (e.g. Figure 1.4), but the hexagonal QR code of GST_{48} , displayed above, is rounded at the corners. We don't know if this is telling us anything about topological properties of GST_{48} .

5.2.2. Fibered Knots. Upon inspecting the values of Θ on the Rolfsen table, Figure 1.1, we noticed that often (but not always) the bar code shows the exact same colour sequence as the top row of the QR code, or exactly its opposite. This and some experimentation lead us to the following conjecture, for which we do not have theoretical support.

Conjecture 17. *If K is a fibered knot and d is the degree of $\Delta(K)$ (the highest power of T), then the coefficient of T_2^{2d} in $\theta(K)$, which is a polynomial in T_1 , is an integer multiple of $T_1^d \Delta(K)|_{T \rightarrow T_1}$. See examples in Figure 5.1, where the integer factor is denoted $s(K)$.*

Using the available fiberedness data in KnotInfo [LM] we found that the condition in this conjecture holds for all 5,397 fibered knots with up to 13 crossings, while it fails on all but 48 of the 7,568 non-fibered knots with up to 13 crossings. See [BV3, FiberedKnots.nb].

We note that if K is fibered then degree d of $\Delta(K)$ is the genus of K , and the coefficient of T^d in $\Delta(K)$ is ± 1 (see [Rol, Section 10H]). The latter condition is an often-used fast-to-compute criterion for a knot to be fibered.

If Conjecture 17 is true then the condition in it is another fast-to-compute criterion for a knot to be fibered, and this criterion is sometimes stronger than the Alexander condition. For example, both the Conway and the Kinoshita-Terasaka knots are not fibered yet their Alexander polynomial is 1, which is monic. In both cases the coefficient of T_2^0 in θ is not an integer multiple of 1 (see Section 3.2), so the condition in Conjecture 17 would detect that these two knots are not fibered.

6. STORIES, CONJECTURES, AND DREAMS

There is a story teller in each of us, who wants to tell a coherent story, with a beginning, a middle, and an end. Unfortunately for us, the Θ story isn't that neat. Calling the content of the first few sections of this paper "the middle", we are quite unsure about the beginning

FIGURE 5.1. The invariant Θ of the fibered knot 12_{n242} , also known as the $(-2, 3, 7)$ pretzel knot, and of the fibered knot 7_7 . For the first, $s(K) > 0$ and the bar code visibly matches with the top row of the QR code (though our screens and printers and eyes may not be good enough to detect minor shading differences, so a visual inspection may not be enough). For the second, twice the degree of Δ is visibly greater than the degree of θ , so $s(K) = 0$.

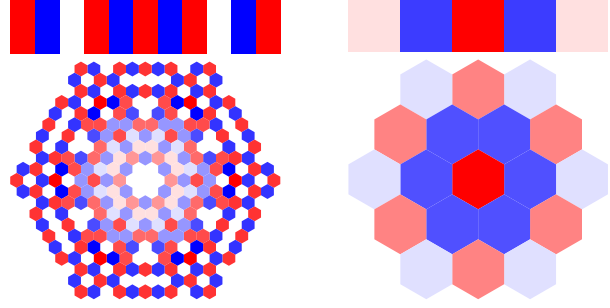
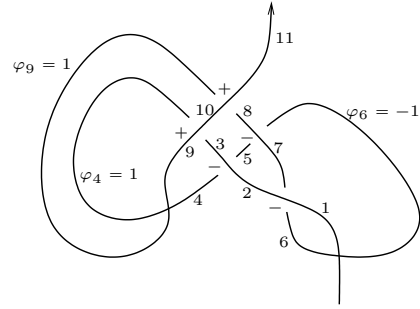


FIGURE 6.1. A long version of the rotational virtual knot KS from [Kau3]. It has $X = \{(-1, 1, 6), (-1, 2, 4), (1, 9, 3), (-1, 7, 5), (1, 10, 8)\}$ and $\varphi = (-1, 0, 0, 1, 0, -1, 0, 0, 1, 0, 0)$.



and the end. The “beginning” can be construed to mean “the thought process that lead us here”. But that process was too long and roundabout to be given in full here (though much of it can be gleaned by reading this section). What’s worse, we believe that ultimately, our peculiar thought process will be replaced by much more solid foundations and motivations, perhaps along the lines of Dreams 31 and 32. But this solid foundation is not available yet, even if we are working hard to expose it. As for the end of the story, it is clearly not known

yet

Hence this section is a bit sketchy and disorganized. Those facts that we already know, those conjectures we believe in, and the dreams we dream, are all here in some random order. But the narrative is lacking.

Conjecture 18. θ has hexagonal symmetry. That is, for any knot K , we have that $\theta = \theta|_{T_1 \rightarrow T_1, T_2 \rightarrow T_1^{-1} T_2^{-1}}$ (“the QR code is invariant under reflection about a horizontal line”), and $\theta = \theta|_{T_1 \rightarrow T_1 T_2, T_2 \rightarrow T_2^{-1}}$ (“the QR code is invariant under reflection about the line of slope 30° ”).



The Alexander polynomial has a simpler symmetry, $\Delta = \Delta|_{T \rightarrow T^{-1}}$. It is rather difficult to deduce the symmetry of Δ from the formula in this paper, Equation (2) (though it is possible; once notational differences are overcome, the proof is e.g. in [CF, Chapter IX]). Instead, the standard proof of the symmetry of Δ uses the Seifert surface formula for Δ (e.g. [Li, Chapter 6]). We expect that Conjecture 18 will be proven as soon as a Seifert formula is found for θ . See Dream 31 below.

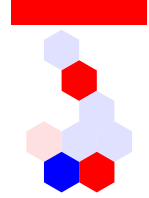
A *rotational virtual knot* is a virtual knot diagram [Kau2] whose edges⁶ are marked with “rotation numbers” φ_k , modulo the same moves as in Figure 4.3.⁷ Clearly, Θ extends to long

⁶Ignoring “virtual crossings”. See [BDV, Section 4].

⁷This definition is slightly different than the original in [Kau3] but the equivalence is easy to show.

rotational virtual knots, and its proof of invariance extends verbatim. Yet as shown below, on the long rotational virtual knot KS of Figure 6.1 (and indeed, on almost any other long rotational virtual knot which is not a classical knot), the hexagonal symmetry of θ fails. So something non-local must happen within any proof of Conjecture 18.

 $KS = \{\{-1, 1, 6\}, \{-1, 2, 4\}, \{1, 9, 3\}, \{-1, 7, 5\}, \{1, 10, 8\}\},$
 $\{0, 0, 0, 1, 0, -1, 0, 0, 1, 0, 0\};$
 PolyPlot[$\theta[KS]$, ImageSize \rightarrow Tiny]



Conjecture 19. If \bar{K} denotes the mirror image of a knot K , then $\theta(\bar{K}) = -\theta(K)$.

Conjecture 20. If $-K$ denotes the reverse of a knot K (namely, K taken with the opposite orientation), then $\theta(-K) = \theta(K)$.

Conjecture 21. θ dominates the Rozansky-Overbay invariant ρ_1 [Roz1, Roz2, Roz3, Ov], also discussed by us in [BV1]. In fact, $\rho_1 = -\theta|_{T_1 \rightarrow T, T_2 \rightarrow 1}$.

Conjecture 22. θ is equal to the “two-loop polynomial” studied extensively by Ohtsuki [Oh2], continuing Rozansky, Garoufalidis, and Kricker [GR, Roz1, Roz2, Roz3, Kr].

Discussion 23. People who are already familiar with “the loop expansion” may consider the above conjecture an “explanation” of θ . We differ. An elementary construction ought to have a simple explanation, and the loop expansion is too complicated to be that.

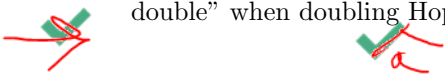
Be it as it may, Ohtsuki [Oh2] shows that Conjecture 22 implies Conjectures 16, 18, 19, and 20. 23

Next, let us briefly sketch some key points from [BN1, BV2], where we explain how to obtain poly-time computable knot invariants from certain Lie algebraic constructions.

Discussion 24. Let \mathfrak{g} be a semi-simple Lie algebra, let \mathfrak{b} be its upper Borel subalgebra, and let \mathfrak{h} be its Cartan subalgebra. Then \mathfrak{b} has a Lie bracket β and, as the dual of the lower Borel subalgebra, it also has a cobracket δ . It turns out that \mathfrak{g} can be recovered from the triple $(\mathfrak{b}, \beta, \delta)$; in fact, $\mathfrak{g}^+ := \mathfrak{g} \oplus \mathfrak{h} \simeq \mathcal{D}(\mathfrak{b}, \beta, \delta)$, where \mathcal{D} denotes the Manin double construction⁸. We now set $\mathfrak{g}_\epsilon^+ := \mathcal{D}(\mathfrak{b}, \beta, \epsilon\delta)$, where ϵ is a formal “small” parameter. The family \mathfrak{g}_ϵ^+ is a 1-parameter family of Lie algebras all defined on the same underlying vector space $\mathfrak{b} \oplus \mathfrak{b}^*$. If ϵ is invertible then \mathfrak{g}_ϵ^+ is independent of ϵ and is always isomorphic to $\mathfrak{g}^+ = \mathfrak{g}_1^+$. Yet at $\epsilon = 0$, \mathfrak{g}_0^+ is solvable, and as the name “solvable” suggests, computations in \mathfrak{g}_0^+ can be “solved”.

Hence in [BN1, BV2], mostly in the case where $\mathfrak{g} = sl_2$, we use the Drinfeld double construction to quantize the universal enveloping algebra $\mathcal{U}(\mathfrak{g}_\epsilon^+)$ and use it to define a “universal quantum invariant” $Z_\epsilon^{\mathfrak{g}}$ (in the sense of [La, Oh1]). We then expand $Z_\epsilon^{\mathfrak{g}}$ near where it’s easy; namely, as a power series around $\epsilon = 0$. In the case of $\mathfrak{g} = sl_2$, and almost certainly in general, we write $Z_\epsilon^{\mathfrak{g}} = \rho_0^{\mathfrak{g}} \exp(\sum_{d \geq 1} \rho_d^{\mathfrak{g}} \epsilon^d)$ and find that we can interpret the $\rho_d^{\mathfrak{g}}$ as polynomials in as many variables as the rank of \mathfrak{g} . It turns out that $\rho_0^{\mathfrak{g}}$ is always determined

⁸We are unsure about naming. \mathcal{D} is also known as “the Drinfeld double” construction for Lie bialgebras (as opposed to Hopf algebras). Yet when Drinfeld first refers to this construction in [Dr], in reference to Lie bialgebras, he repeatedly names it after Manin (under the less clear name “Manin triples”), yet without providing a reference. Our choice is to use “Manin double” when doubling Lie bialgebras and “Drinfeld double” when doubling Hopf algebra, as we found no indication that Manin knew about the latter process.



by the Alexander polynomial and the $\rho_d^{\mathfrak{g}}$ are always computable in polynomial time (with polynomials whose exponents and coefficients get worse as d grows bigger and \mathfrak{g} gets more complicated.)

Our papers and talks [BV1, BV2, BN3] carry out the above procedure in the case where $\mathfrak{g} = sl_2$, calling the resulting invariants ρ_d , for $d \geq 1$. They are the same as ρ_1 and ρ_2 of Section 5.1. 24

Following some preliminary work by Schaveling [Sch], in the summer of 2024 we've set out to find good formulas for $\rho_1^{sl_3}$. Tracing Discussion 24 seemed technically hard, so instead, we extracted from the procedure the “shape” of the formulas we could expect to get and, and then we found the invariant θ by the method of undetermined coefficients assisted by some difficult-to-formulate intuition (more in Comment 30 below). Thus our formulas for θ arose from our expectations for $\rho_1^{sl_3}$, and yet we have not proved that they are equal!

Conjecture 25. *Up to conventions and normalizations, $\theta = \rho_1^{sl_3}$.*

Comment 26. Using the techniques of [BN2, BV2] we expect to be able to prove a genus bound for $\rho_1^{sl_3}$, similar to the bound in Conjecture 16. Thus we expect that Conjecture 25 will imply Conjecture 16.

Discussion 27. People who are versed with Lie algebras and their quantizations may consider the above an “explanation” of θ , and may be looking forward to a more detailed exposition of $\rho_d^{\mathfrak{g}}$. We differ, for the same reasons as in Discussion 23. We expect the eventual “origin story” for θ to be simpler and more natural. 27

Discussion 28. It is the basis of the theory of “Feynman diagrams”, and hence it is extremely well known in the physics community, that perturbed Gaussian integrals, when convergent, can be computed (as asymptotic series) efficiently using “Feynman diagrams” (see e.g. [Po1]). Physicists use this routinely in infinite dimensions; yet the finite dimensional formulation can be sketched as follows:

$$\int_{\mathbb{R}^d} e^{Q+\epsilon P} \sim C \sum_{n \geq 0} \epsilon^n \sum_F \mathcal{E}(F), \quad (19)$$

where Q is a non-degenerate quadratic on \mathbb{R}^d , P is a “smaller” perturbation, C is some constant involving π 's and the determinant of Q , the summation \sum_F is over “Feynman diagrams” of complexity n , and $F \mapsto \mathcal{E}(F)$ is some procedure, which can be specified in full but we will not do it here, which assigns to every Feynman diagram F an algebraic sum which in itself depends only on the coefficients of P and the entries of the inverse of Q .

In fact, one may take the right-hand-side of Equation (19) to be the definition of the left-hand-side, especially if the left-hand-side is not convergent, or does not make sense for some other reason. Namely, one may set

$$\oint_{\mathbb{R}^d} e^{Q+\epsilon P} := C \sum_{n \geq 0} \epsilon^n \sum_F \mathcal{E}(F). \quad (20)$$

The result is an integration theory defined on perturbed Gaussians in fully algebraic terms, and which shares some of the properties of “ordinary” integration, such as having a version of Fubini's theorem. In a sense, that's what physicists do: path integrals don't quite make sense, so instead they are defined using Feynman diagrams and the right-hand-side of Equation (20). Another example is the “Århus integral” of [BGRT], where the integral in itself is diagrammatic, as is the output of the integration procedure. 28

Fact 29. *There is a perturbed Gaussian formula for Θ . More precisely, one can assign a 6-dimensional Euclidean space \mathbb{R}_e^6 with coordinates $p_{1e}, p_{2e}, p_{3e}, x_{1e}, x_{2e}, x_{3e}$ to each edge e of a knot diagram D and then form $\mathbb{R}_{6E} := \prod_e \mathbb{R}_e^6$, a space whose dimension is 6 times the number of edges in E . One can then form a “Lagrangian” $L_D = Q_D + \epsilon P_D$ by summing over all the crossings of D local contributions that involve only the variables associated with the four edges around each crossings, and adding a “correction” which is a sum over the edges e of D of terms that depend only on the rotation number of e and on the variables in \mathbb{R}_e^6 , such that*

$$\oint_{\mathbb{R}_{6E}} e^{L_D} = \oint_{\mathbb{R}_{6E}} e^{Q_D + \epsilon P_D} = \frac{(2\pi)^{3|E|}}{\Delta_1 \Delta_2 \Delta_3} \exp\left(\epsilon \frac{\theta}{\Delta_1 \Delta_2 \Delta_3}\right) + O(\epsilon^2),$$

and such that the Feynman diagram expansion of the left-hand-side of the above equation becomes precisely formula (6) for θ . See more about all this in [BN5].

Comment 30. In fact, Fact 29 is what we initially predicted based on Discussion 24, along with some further information about the “shape” of P_D . We used the method of undetermined coefficients to find precise formulas for P_D , and then the technique of Feynman diagrams to derive our main formula, Equation 6.

Dream 31. *There is a “Seifert formula” for Θ . More precisely, let K be a knot, let Σ be a Seifert surface for K , let $H := H_1(\Sigma; \mathbb{R})$, and let $6H$ denote $H \oplus H \oplus H \oplus H \oplus H \oplus H$. Let Q_Σ denote 3 copies of the standard Seifert form on $H \oplus H$, taken with parameters T_1, T_2 , and T_3 ; so Q_Σ is a quadratic on $6H$. We dream that there a “perturbation term” P_Σ , a polynomial function on $6H$ defined in terms of some low degree finite type invariants of various knotted graphs formed by representatives of classes in H (also taking account of their intersections), such that*

$$\oint_{6H} e^{L_\Sigma} = \oint_{6H} e^{Q_\Sigma + \epsilon P_\Sigma} = \frac{(2\pi)^{3 \dim(H)}}{\Delta_1 \Delta_2 \Delta_3} \exp\left(\epsilon \frac{\theta}{\Delta_1 \Delta_2 \Delta_3}\right) + O(\epsilon^2).$$

If this dream is true, it will probably prove Conjectures 16, 18, 19, and 20 much as the Seifert formula for Δ can be used to prove the genus bound provided by Δ and its basic symmetry properties.

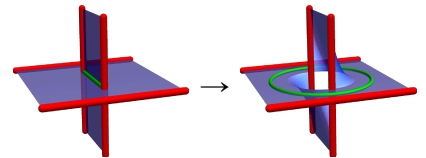
We note the relationship between this dream and [Oh2, Theorem 4.4].

Dream 32. *All the invariants from Discussion 24 have Seifert formulas in the style of Dream 31. In fact, there ought to be a characterization of those Lagrangians L_Σ for which $\oint e^{L_\Sigma}$ is a knot invariant, and there may be a construction of all those Lagrangians which is intrinsic to topology and does not rely of the theory of Lie algebras.*

If a knot K is ribbon then for some g it has a Seifert surface Σ of genus g such that g of the generators of $H_1(\Sigma)$ can be represented by a g -component unlink (see the hint on the right, and see further details in [Kau1, Chapter VIII] or in [Ba, Section 3.4]). This implies that the Seifert matrix

M of Σ has the form $\begin{pmatrix} 0 & A \\ A^* & B \end{pmatrix}$, which implies that the determinant of M , the Alexander polynomial Δ , satisfies the Fox-Milnor condition:

Theorem 33 (Fox and Milnor, [FM]). *If K is a ribbon knot, then there exists some polynomial $f(T)$ such that $\Delta = f(T)f(T^{-1})$.*



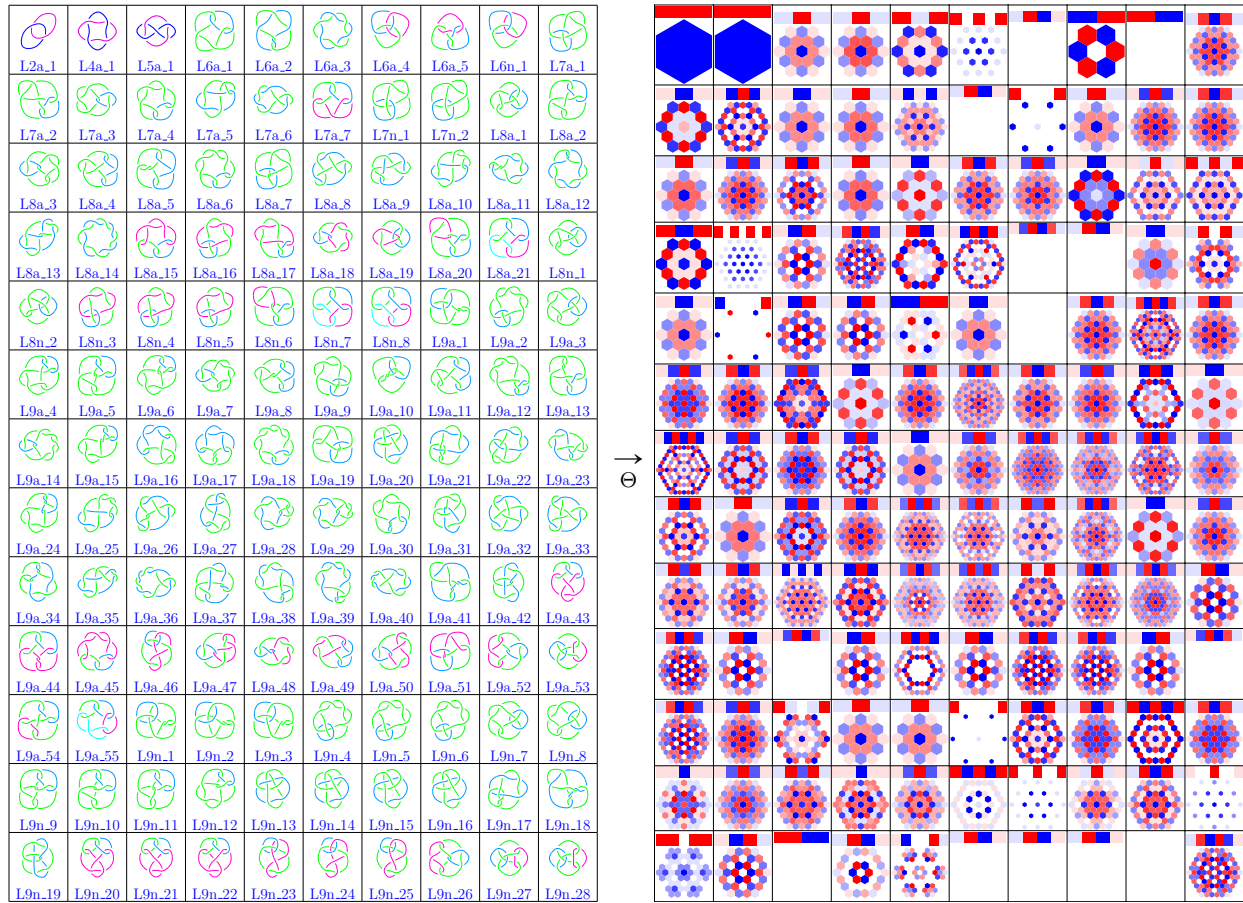


FIGURE 6.2. Θ for all the prime links with up to 9 crossings, up to reflections and with arbitrary choices of strand orientations. Empty boxes correspond to links for which $\Delta = 0$.

Dream 34. *Dream 31, along with the fact that half the homology of a Seifert surface of a ribbon knot can be represented by an unlink, will imply that θ takes a special form on ribbon knots, giving us stronger powers to detect knots that are not ribbon.*

Discussion 35. In this paper we concentrated on knots, yet at least partially, Θ can be generalized also to links. Indeed, the definitions in Section 2 and the proof in Section 4 go through provided the matrix A is invertible; namely, provided the Alexander polynomial Δ is non-zero (for knots, this is always the case), and provided we choose one component of the link to cut open.

The programs of Section 3 fail for minor reasons, and a fix is in [BV3, Theta4Links.nb]. Some results are in Figure 6.2. Preliminary testing using these programs suggests that the resulting invariant is independent of the choice of the cut component, but we did not prove that.

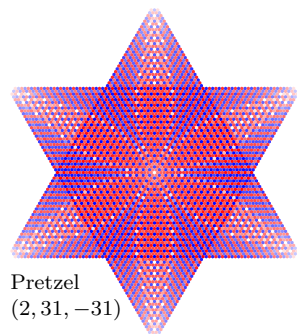
If $\Delta = 0$, one may contemplate replacing $G = A^{-1}$ by the adjugate matrix $\text{adj}(A)$ of A (the matrix of codimension 1 minors, which satisfies $A \cdot \text{adj}(A) = \det(A)I$). Some preliminary testing is also in [BV3, Theta4Links.nb]. Yet if G is replaced with $\text{adj}(A)$, its equivalence with the g -rules (Equations (8) and (9)) breaks, and so we have no proof of invariance. We may attempt to fix that in a future work, but it is not done yet.

→ We note that the ~~two~~ loop expansion of Conjecture 22 does not predict that Θ should extend to links. We also note that the solvable approximation technique of Discussion 24 does predict that ~~extension~~, and in fact, it predicts more: that much like the Gassner representation [Ga] and the multi-variable Alexander polynomial (e.g. [Kaw, Chapter 7]), there should be a multi-variable version of Θ which would be a polynomial in $2m$ variables when evaluated on an m -component link. We did not attempt to find explicit formulas for the multi-variable Θ . 35

REFERENCES

- [Al] J. W. Alexander, *Topological invariants of knots and link*, Trans. Amer. Math. Soc. **30** (1928) 275–306. See pp. 2.
- [Ba] S. Bai, *Alexander Polynomials of Ribbon Knots and Virtual Knots*, [arXiv:2103.07128](https://arxiv.org/abs/2103.07128). See pp. 28.
- [BN1] D. Bar-Natan, *Everything around sl_{2+}^{ϵ} is DoPeGDO. So what?*, talk given in “Quantum Topology and Hyperbolic Geometry Conference”, Da Nang, Vietnam, May 2019. Handout and video at [omega-beta/DPG](https://www.drorbn.net/omega-beta/DPG). See pp. 26.
- [BN2] D. Bar-Natan, *Algebraic Knot Theory*, talk given in Sydney, September 2019. Handout and video at [omega-beta/AKT](https://www.drorbn.net/omega-beta/AKT). See pp. 27.
- [BN3] D. Bar-Natan, *Cars, Interchanges, Traffic Counters, and some Pretty Darned Good Knot Invariants*, talk given in Oaxaca, October 2022. Video and handout at <http://drorbn.net/oa22>. See pp. 14, 23, 27.
- [BN4] D. Bar-Natan, *Shifted Partial Quadratics, their Pushforwards, and Signature Invariants for Tangles*, talk given in Geneva, December 2023. Video and handout at <http://drorbn.net/ge23>. See pp. 22.
- [BN5] D. Bar-Natan, *Knot Invariants from Finite Dimensional Integration*, talks in Beijing (July 2024, <http://drorbn.net/icbs24>), Geneva (August 2024, <http://drorbn.net/ge24>) and Bonn (May 2025, <http://drorbn.net/bo25>). See pp. 6, 7, 28.
- [BN6] D. Bar-Natan, *The Strongest Genuinely Computable Knot Invariant in 2024*, talk given in Toronto (October 2024, <http://drorbn.net/to24>). See pp. 6, 14.
- [BDV] D. Bar-Natan, Z. Dancso and R. van der Veen, *Over then Under Tangles*, J. of Knot Theory and its Ramifications **32-8** (2023), [arXiv:2007.09828](https://arxiv.org/abs/2007.09828). See pp. 25.
- [BGRT] D. Bar-Natan, S. Garoufalidis, L. Rozansky, and D. P. Thurston, *The Århus integral of rational homology 3-spheres I–III*, Selecta Math., New Series **8** (2002) 315–339, [arXiv:q-alg/9706004](https://arxiv.org/abs/q-alg/9706004), **8** (2002) 341–371, [arXiv:math.QA/9801049](https://arxiv.org/abs/math.QA/9801049), **10** (2004) 305–324, [arXiv:math.QA/9808013](https://arxiv.org/abs/math.QA/9808013). See pp. 27.
- [BV1] D. Bar-Natan and R. van der Veen, *A Perturbed-Alexander Invariant*, Quantum Topology **15** (2024) 449–472, [arXiv:2206.12298](https://arxiv.org/abs/2206.12298). See pp. 6, 7, 12, 13, 14, 23, 26, 27.
- [BV2] D. Bar-Natan and R. van der Veen, *Perturbed Gaussian Generating Functions for Universal Knot Invariants*, [arXiv:2109.02057](https://arxiv.org/abs/2109.02057). See pp. 26, 27.
- [BV3] D. Bar-Natan and R. van der Veen, *A Fast, Strong, Topologically Meaningful, and Fun Knot Invariant*, (self-reference), paper and related files at <http://drorbn.net/Theta>. The [arXiv:????](https://arxiv.org/abs/????) edition may be older. See pp. 4, 8, 11, 22, 23, 24, 29.
- [BVH] J. Bécerra and K. van Helden, *Minimal Generating Sets of Rotational Reidemeister Moves*, [arXiv:2506.15628](https://arxiv.org/abs/2506.15628). See pp. 16.
- [Co] A. Conway, *The Levine-Tristram Signature: A Survey*, in 2019–20 MATRIX Annals, Springer 2021, [arXiv:1903.04477](https://arxiv.org/abs/1903.04477). See pp. 22.
- [CF] R. H. Crowell and R. H. Fox, *Introduction to Knot Theory*, Springer-Verlag GTM **57** (1963). See pp. 25.
- [CDGW] M. Culler, N. Dunfield, M. Goerner, and J. Weeks, *SnapPy, a computer program for studying the geometry and topology of 3-manifolds*, <http://snappy.computop.org>. See pp. 22.
- [Dr] V. G. Drinfel’d, *Quantum Groups*, Proc. Int. Cong. Math., 798–820, Berkeley, 1986. See pp. 26.
- [DHOEBL] N. Dunfield, A. Hirani, M. Obeidin, A. Ehrenberg, S. Bhattacharyya, D. Lei, and others, *Random Knots: A Preliminary Report*, lecture notes at https://nmd.web.illinois.edu/slides/random_knots.pdf. Also a data file at https://drorbn.net/AcademicPensieve/People/Dunfield/nmd_random_knots. See pp. 5.

- [FM] R. H. Fox and J. W. Milnor, *Singularities of 2-Spheres in 4-Space and Cobordism of Knots*, Osaka J. Math. **3-2** (1966) 257–267. See pp. 28.
- [Ga] B. J. Gassner, *On Braid Groups*, Ph.D. thesis, New York Univeristy, 1959. See pp. 30.
- [GK] S. Garoufalidis and R. Kashaev, *Multivariable Knot Polynomials from Braided Hopf Algebras with Automorphisms*, [arXiv:2311.11528](https://arxiv.org/abs/2311.11528). See pp. 23.
- [GL] S. Garoufalidis and S. Y. Li, *Patterns of the V_2 -Polynomial of Knots*, [arXiv:2409.03557](https://arxiv.org/abs/2409.03557). See pp. 23.
- [GR] S. Garoufalidis and L. Rozansky, *The Loop Expansion of the Kontsevich Integral, the Null-Move, and S-Equivalence*, [arXiv:math.GT/0003187](https://arxiv.org/abs/math.GT/0003187). See pp. 1, 26.
- [GST] R. E. Gompf, M. Scharlemann, and A. Thompson, *Fibered Knots and Potential Counterexamples to the Property 2R and Slice-Ribbon Conjectures*, Geom. and Top. **14** (2010) 2305–2347, [arXiv:1103.1601](https://arxiv.org/abs/1103.1601). See pp. 23, 24.
- [Kau1] L. H. Kauffman, *On knots*, Princeton Univ. Press, Princeton, 1987. See pp. 28.
- [Kau2] L. H. Kauffman, *Virtual Knot Theory*, European J. Comb. **20** (1999) 663–690, [arXiv:math.GT/9811028](https://arxiv.org/abs/math.GT/9811028). See pp. 25.
- [Kau3] L. H. Kauffman, *Rotational Virtual Knots and Quantum Link Invariants*, J. of Knot Theory and its Ramifications **24-13** (2015), [arXiv:1509.00578](https://arxiv.org/abs/1509.00578). See pp. 25.
- [Kaw] A. Kawauchi, *A Survey of Knot Theory*, Birkhauser Verlag, 1996. See pp. 30.
- [Kr] A. Kriker, *The Lines of the Kontsevich Integral and Rozansky’s Rationality Conjecture*, [arXiv:math/0005284](https://arxiv.org/abs/math/0005284). See pp. 1, 26.
- [La] R. J. Lawrence, *Universal Link Invariants using Quantum Groups*, Proc. XVII Int. Conf. on Diff. Geom. Methods in Theor. Phys., Chester, England, August 1988. World Scientific (1989) 55–63. See pp. 26.
- [Le] J. Levine, *Knot cobordism groups in codimension two*, Comment. Math. Helv. **44** (1969) 229–244. See pp. 22.
- [Li] W. B. R. Lickorish, *An Introduction to Knot Theory*, Springer-Verlag GTM **175** (1997). See pp. 25.
- [LM] C. Livingston and A. H. Moore, *KnotInfo: Table of Knot Invariants*, <http://knotinfo.org>, August 26, 2025. See pp. 23, 24.
- [Oh1] T. Ohtsuki, *Quantum Invariants*, Series on Knots and Everything **29**, World Scientific 2002. See pp. 26.
- [Oh2] T. Ohtsuki, *On the 2-Loop Polynomial of Knots*, Geometry & Topology **11** (2007) 1357–1475. See pp. 1, 26, 28.
- [Ov] A. Overbay, *Perturbative Expansion of the Colored Jones Polynomial*, Ph.D. thesis, University of North Carolina, August 2013, <https://cdr.lib.unc.edu/concern/dissertations/hm50ts889>. See pp. 23, 26.
- [Po1] M. Polyak, *Feynman Diagrams for Pedestrians and Mathematicians*, [arXiv:math/0406251](https://arxiv.org/abs/math/0406251). See pp. 27.
- [Po2] M. Polyak, *Minimal Generating Sets of Reidemeister Moves*, Quantum Topol. **1** (2010) 399–411, [arXiv:0908.3127](https://arxiv.org/abs/0908.3127). See pp. 14.
- [Rol] D. Rolfsen, *Knots and Links*, AMS Chelsea, 2003. See pp. 24.
- [Roz1] L. Rozansky, *A Contribution of the Trivial Flat Connection to the Jones Polynomial and Witten’s Invariant of 3D Manifolds, I*, Comm. Math. Phys. **175-2** (1996) 275–296, [arXiv:hep-th/9401061](https://arxiv.org/abs/hep-th/9401061). See pp. 1, 23, 26.
- [Roz2] L. Rozansky, *The Universal R-Matrix, Burau Representation and the Melvin-Morton Expansion of the Colored Jones Polynomial*, Adv. Math. **134-1** (1998) 1–31, [arXiv:q-alg/9604005](https://arxiv.org/abs/q-alg/9604005). See pp. 1, 23, 26.
- [Roz3] L. Rozansky, *A Universal $U(1)$ -RCC Invariant of Links and Rationality Conjecture*, [arXiv:math/0201139](https://arxiv.org/abs/math/0201139). See pp. 1, 23, 26.
- [Sch] S. Schaveling, *Expansions of Quantum Group Invariants*, Ph.D. thesis, Universiteit Leiden, September 2020, <https://scholarlypublications.universiteitleiden.nl/handle/1887/136272>. See pp. 27.
- [Tr] A. Tristram, *Some cobordism invariants for links*, Proc. Cambridge Philos. Soc. **66** (1969) 251–264. See pp. 22.
- [Wo] *Wolfram Language & System Documentation Center*, <https://reference.wolfram.com/language/>. See pp. 8.



Pretzel
(2, 31, -31)

DEPARTMENT OF MATHEMATICS, UNIVERSITY OF TORONTO, TORONTO
ONTARIO M5S 2E4, CANADA

Email address: drorbn@math.toronto.edu

URL: <http://www.math.toronto.edu/drorbn>

UNIVERSITY OF GRONINGEN, BERNOULLI INSTITUTE, P.O. Box 407, 9700
AK GRONINGEN, THE NETHERLANDS

Email address: roland.mathematics@gmail.com

URL: <http://www.rolandvdv.nl/>